Talos: Optimizing Top-K Accuracy in Recommender Systems

Shengjia Zhang[†‡§]
Zhejiang University
Hangzhou, China
shengjia.zhang@zju.edu.cn

Weiqin Yang[†‡§]
Zhejiang University
Hangzhou, China
tinysnow@zju.edu.cn

Jiawei Chen[*‡§¶]
Zhejiang University
Hangzhou, China
sleepyhunt@zju.edu.cn

Peng Wu[‖]
Beijing Technology and Business
University
Beijing, China
pengwu@btbu.edu.cn

Yuegang Sun
Intelligence Indeed
Hangzhou, China
bulutuo@i-i.ai

Gang Wang
Bangsheng Technology Co,Ltd.
Hangzhou, China
wanggang@bsfit.com.cn

Qihao Shi
Hangzhou City University
Hangzhou, China
shiqihao321@zju.edu.cn

Can Wang[‡¶]
Zhejiang University
Hangzhou, China
wcan@zju.edu.cn

Abstract

Recommender systems (RS) aim to retrieve a small set of items that best match individual user preferences. Naturally, RS place primary emphasis on the quality of the Top-K results rather than performance across the entire item set. However, estimating Top-K accuracy (*e.g.,* Precision@K, Recall@K) requires determining the ranking positions of items, which imposes substantial computational overhead and poses significant challenges for optimization. In addition, RS often suffer from distribution shifts due to evolving user preferences or data biases, further complicating the task.

To address these issues, we propose Talos, a loss function that is specifically designed to optimize the Top-K recommendation accuracy. Talos leverages a quantile technique that replaces the complex ranking-dependent operations into simpler comparisons between predicted scores and learned score thresholds. We further develop a sampling-based regression algorithm for efficient and accurate threshold estimation, and introduce a constraint term to maintain optimization stability by preventing score inflation. Additionally, we incorporate a tailored surrogate function to address discontinuity and enhance robustness against distribution shifts. Comprehensive theoretical analyzes and empirical experiments are conducted to demonstrate the effectiveness, efficiency, convergence, and distributional robustness of Talos. The code is available at https://github.com/cynthia-shengjia/WWW-2026-Talos.

CCS Concepts

- **Information systems → Recommender systems**.

Keywords

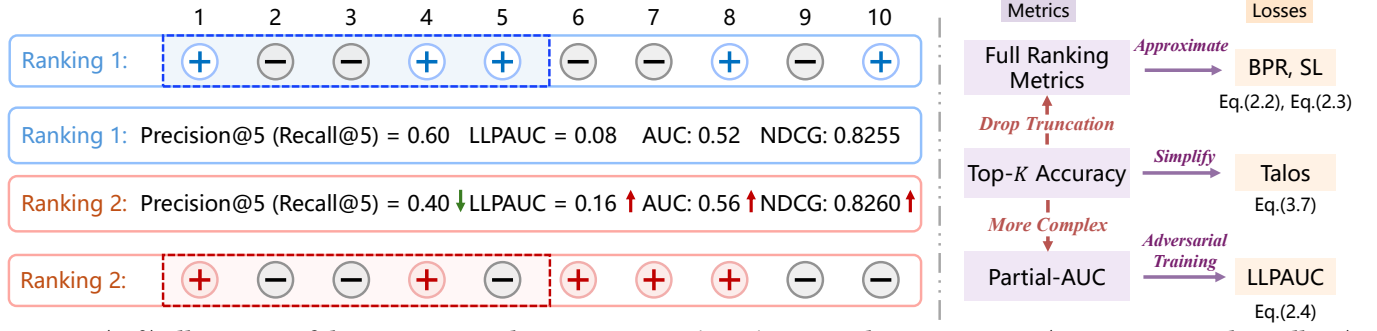Recommender Systems, Top-K Accuracy, Loss Functions

1 Introduction

Being able to provide personalized suggestions, Recommender Systems (RS) [24, 64] are integral to several online service platforms. On these platforms, users are typically presented with only a small set of items. Consequently, RS primarily emphasizes the quality of the Top-K items (*e.g.,* Precision@K and Recall@K) rather than the performance across the entire item set. Existing RS often adopt a learning-based paradigm [16, 53] — learning a recommendation model to estimate user preference scores over items and then retrieving the Top-K items with the highest predicted scores as recommendations.

The distinct focus on Top-K accuracy has inspired extensive research on recommendation loss functions. The loss function determines the direction of model optimization, whose importance cannot be overemphasized [54, 57]. Recent years have witnessed the emergence of two prominent types of loss functions:

- **Full-ranking Losses**: Some works aim to improve the overall ranking performance without explicitly targeting Top-K estimation. Prominent examples include BPR [38] and Softmax Losses [54], which have been shown to approximately optimize the Area Under the ROC Curve (AUC) and Normalized Discounted Cumulative Gain (NDCG), respectively. However, AUC and NDCG evaluate the quality of the entire ranking list, which can differ substantially from the quality of the Top-K subset

Figure 1: (*Left*). Illustration of the inconsistency between LLPAUC/AUC/NDCG and Top-K accuracy (Precision@K and Recall@K) for two difference ranking schemes of ten items, where ranking scheme 2 achieves better AUC/LLPAUC and NDCG, while worse on Top-K accuracy; (*Right*). The relationship among Talos, LLPAUC, SL, and BPR.

most relevant to RS outcomes. Consequently, optimizing these full-ranking loss functions does not necessarily translate to improvements in Top-K accuracy and may sometimes reduce it. Figure 1 provides an example where AUC and NDCG increase while Precision@K and Recall@K decrease. Such cases are not rare in RS. By empirically analyzing arbitrary pairs of ranking lists for users on real-world datasets, we observe that the ratio of such inconsistent cases exceeds 34.37% and 28.49% on average.

- **Partial-AUC-based Losses**: Another line of research focuses on developing loss functions for optimizing Partial-AUC metrics (*e.g.,* LLPAUC [43] and OPAUC [42]), which evaluate the partial area under the ROC curve and correlate more strongly with Top-K accuracy than full-ranking losses. Indeed, as shown in Table 1.1, the inconsistency ratio between LLPAUC and Precision@K decreases to 21.86% on average. Nevertheless, the gap still exists. More critically, Partial-AUC metrics are highly complex, incurring significant optimization challenges. It can be seen from their surrogate loss functions often involve adversarial training [43], which complicates training stability and reduces effectiveness. Furthermore, these loss functions introduce additional hyperparameters compared to BPR and SL, necessitating expensive and time-consuming tuning efforts. These limitations significantly hinder their practical application.

Given these limitations, an important research question raises: *How can we design a loss function that directly optimizes top-K accuracy in recommender systems?* Considering the characteristics of Top-K optimization and RS, we identify the following key obstacles:

- **Ranking-aware Discontinuous Objective**: Top-K accuracy (*e.g.,* Precision@K) are computed only over the Top-K ranked items, requiring a ranking-dependent truncation — determining which items lie in the Top-K positions. This process requires computing item ranking positions, incurring high computational cost. It also makes the objective discontinuous or constant in large regions, making gradient-based optimization ineffective.
- **Distributional-Shift Challenge:** It is important to note that RS often faces severe distribution shifts due to evolving user preference [50] or data collection biases [3, 4, 12, 27]. Loss functions that are robust to such shifts have been shown to be essential for RS performance [53].

To address these challenges, we propose Talos, a new loss function specifically designed for optimizing Top-K recommendation accuracy (*e.g.,* Precision@K and Recall@K). To overcome the ranking-dependence, we introduce the quantile [13, 25, 40] to reformulate Top-K selection into simple comparisons between item scores and a learned score threshold. Items with scores above the threshold constitute the Top-K, avoiding explicit sorting and thus significantly facilitating optimization. However, this threshold-based strategy also raises two further questions: 1) **Threshold estimation**: The valid thresholds vary per user, requiring efficient and accurate estimation; 2) **Convergence concern**: Thresholds evolve during training, raising concerns about training convergence and stability. Particularly, we observe score inflation phenomenon that both predicted scores and thresholds rise excessively. We resolve these by: 1) Developing a sampling-based quantile regression method for fast and accurate estimation; 2) Introducing a constraint term limiting the number of items above the threshold, ensuring training convergence and stability.

Additionally, to further tackle discontinuity and distribution shift, we design a specific smooth surrogate function approximating the Heaviside step function. These designs endow Talos with three fundamental theoretical properties: 1) Talos serves as a tight upper bound for optimizing Precision@K, ensuring its effectiveness; 2) Talos is equivalent to performing *Distributionally Robust Optimization*, a theoretical-sound approach that empowers the model with robustness against distribution shifts; 3) the optimization procedure for Talos provides theoretically convergence guarantees.

The proposed Talos is practical in three aspects: 1) It is concise in form and can be easily plug-in existing RS models with minimal code modifications; 2) It is computationally efficient, with both theoretical time complexity and practical runtime comparable to the conventional loss; 3) It preserves simplicity in hyperparameter tuning, requiring only a single temperature parameter. In summary, our main contributions are:

- We propose Talos, a novel loss function for directly optimizing Top-K recommendation accuracy.
- We provide comprehensive theoretical analyses, demonstrating its effectiveness, distributional robustness, and convergence guarantees.
- We conduct extensive experiments across four datasets and three backbone models, verifying the superiority of Talos over the state-of-the-art losses.

Table 1.1: Empirical analyses of the inconsistency between AUC/LLPAUC/NDCG/NDCG@*K* and Top-*K* accuracy across arbitrary pairs of ranking lists on real-world datasets.

Metric	Gowalla		Beauty		Games		Electronics	
	Precision@20	Recall@20	Precision@20	Recall@20	Precision@20	Recall@20	Precision@20	Recall@20
AUC	33.17%	33.89%	34.67%	35.46%	35.17%	34.19%	33.32%	34.58%
LLPAUC	18.53%	18.65%	23.81%	22.95%	23.30%	22.34%	23.30%	22.25%
NDCG	26.70%	26.88%	29.65%	29.52%	29.52%	28.02%	29.11%	28.53%
NDCG@*K*	19.01%	18.24%	22.02%	22.55%	21.14%	22.21%	17.65%	17.51%

2 Preliminaries

In this section, we present the task formulation, an overview of the Top-*K* accuracy and an analysis of existing loss functions.

2.1 Task Formulation

Aligned with recent studies [17, 44] on recommendation losses, this work focuses on the conventional collaborative filtering (CF) scenario. Let $\mathcal{U}$ and $\mathcal{I}$ denote the sets of users and items, respectively. The set of observed interactions is represented as $\mathcal{D} \subseteq \mathcal{U} \times \mathcal{I}$, where each entry $(u, i) \in \mathcal{D}$ signifies an interaction (*e.g.,* click, purchase, etc) between user u and item i. Consequently, for a given user u, the positive item set $\mathcal{P}_u = \{i \in \mathcal{I} : (u, i) \in \mathcal{D}\}$ is constructed from the observed interactions, while the remaining unobserved items constitute the negative item set $\mathcal{N}_u = \mathcal{I} \setminus \mathcal{P}_u$. The primary objective of recommender systems is to leverage the historical data $\mathcal{D}$ to predict the Top-*K* items that best match the user's preferences.

Existing RS mainly adopt a learning-based paradigm [17]. Specifically, a parameterized recommendation model M_θ takes the features (*e.g.,* IDs) of user u and item i as input [58] to generate the preference scores $s_{ui} = M_\theta(u, i)$. The model is then optimized from $\mathcal{D}$ under a specific loss function. Ultimately, the recommendation list for user u is generated by ranking items according to s_{ui} and retaining the Top-*K* candidates. Thus, the loss function, which governs the optimization trajectory of the model, plays a crucial role in RS.

2.2 Top-*K* Accuracy in RS

As RS typically display only the Top-*K* items to users, Top-*K* accuracy, *e.g.,* Precision@*K* and Recall@*K*, are commonly used to evaluate the recommendation performance, which are defined as

$$\text{Precision@}K(u) = \sum_{i \in \mathcal{P}_u} \frac{\mathbb{I}(\pi_{ui} \leq K)}{K}, \ \text{Recall@}K(u) = \sum_{i \in \mathcal{P}_u} \frac{\mathbb{I}(\pi_{ui} \leq K)}{|\mathcal{P}_u|}$$
(2.1)

where $\mathbb{I}(\cdot)$ denotes the indicator function, $\pi_{ui} = \sum_{j \in \mathcal{I}} \mathbb{I}(s_{uj} \geq s_{ui})$ denotes the ranking position of item i for user u. These metrics measure the the quality (positivity) of the top-ranked items, and incorporate a ranking-dependent truncation term $\mathbb{I}(\pi_{ui} \leq K)$ that determines whether an item ranks within the Top-*K*. Notably, this study primarily targets the optimization of Top-*K* accuracy, *i.e.,* Precision@*K* and Recall@*K*. Although more sophisticated metrics (*e.g.,* NDCG@*K*, MRR@*K*) additionally capture position-aware relevance, they are not as prevalent as Precision@*K* and Recall@*K* in modern RS. Precision@*K* and Recall@*K* exhibit a more direct correlation with online business-critical metrics [8, 35, 65] (*e.g.,* CTR), and are widely regarded as gold-standard indicators for the recall stage of recommendation pipelines [37, 63]. Furthermore, since complex metrics are on the basis of Top-*K* accuracy, improving Top-*K*

accuracy can potentially enhance these metrics, as evidenced by the results reported in Appendix E.

2.3 Analyses on Existing Loss Functions

Beyond the traditional point-wise and pair-wise loss functions [22, 33, 38], recent years have witnessed the emergence of two prominent types of loss function in RS:

Full Ranking Losses. The most prominent examples that optimize the full ranking metrics are BPR and Softmax Loss (SL). BPR is a surrogate loss that is defined as:

$$\mathcal{L}_{\text{BPR}} = \frac{1}{|\mathcal{P}_u|} \sum_{i \in \mathcal{P}_u} \sum_{j \in \mathcal{N}_u} \log \sigma(s_{uj} - s_{ui}), \ \text{AUC} = \sum_{i \in \mathcal{P}_u} \sum_{j \in \mathcal{N}_u} \frac{\mathbb{I}(s_{ui} \geq s_{uj})}{|\mathcal{P}_u||\mathcal{N}_u|}$$
(2.2)

where σ seeks to approximate the Heaviside function, typically set as the sigmoid function [38]. Consequently, BPR loss serves as an approximation of AUC metric. For each user, SL [54] is defined as:

$$\mathcal{L}_{\text{SL}} = -\frac{1}{|\mathcal{P}_u|} \sum_{i \in \mathcal{P}_u} \log \frac{\exp(s_{ui}/\tau)}{\sum_{j \in \mathcal{I}} \exp(s_{uj}/\tau)}$$
(2.3)

where τ serves as a temperature hyperparameter. Recent theoretical analysis [57] have demonstrated that SL as a tight surrogate loss for optimizing the full-ranking metric NDCG. This property often allows SL to yield state-of-the-art performance.

However, we argue that the full-ranking metrics differ significantly from Top-*K* accuracy. This discrepancy is evident as Top-*K* accuracy incorporate a truncation term $\mathbb{I}(\pi_{ui} \leq K)$, indicating that performance is evaluated only on Top-*K* items. To further illustrate this difference, we conduct an empirical analysis (see Appendix D.1 for details). As shown in Table 1.1, the deviation between NDCG and Top-*K* accuracy significantly exceeds 20.47% on average. These results suggest that optimizing NDCG may not always lead to better Top-*K* accuracy and, in some cases, may even degrade performance. As shown in Table 1.1, the deviation between NDCG and Top-*K* accuracy is significant (20.47% on average).

Partial-AUC-based Losses. Another research line focuses on optimizing Partial-AUC metrics [42, 67], which quantify the area under a specific segment of the ROC curve. The general Partial-AUC metric, Lower-Left Partial AUC (LLPAUC), is formally defined as [43]:

$$\text{LLPAUC} = \sum_{i \in \mathcal{P}_u} \sum_{j \in \mathcal{N}_u} \frac{\mathbb{I}(s_{ui} \geq s_{uj}) \cdot \mathbb{I}(s_{ui} \geq \eta_\alpha) \cdot \mathbb{I}(s_{uj} \geq \eta_\beta)}{|\mathcal{P}_u||\mathcal{N}_u|}$$
(2.4)

s.t. $\mathbf{Pr}_{i \sim U(\mathcal{P}_u)}[s_{ui} \geq \eta_\alpha] = \alpha$ and $\mathbf{Pr}_{j \sim U(\mathcal{N}_u)}[s_{uj} \geq \eta_\beta] = \beta$

where η_α and η_β denote the hyperparameters that delineate the evaluation region, $U(\cdot)$ denotes the uniform distribution. Compared to the original AUC, constraints in Eq.(2.4) are introduced, evaluating ranking performance on positive and negative items with

Shengjia Zhang, Weiqin Yang, Jiawei Chen, Peng Wu, Yuegang Sun, Gang Wang, Qihao Shi, and Can Wang

high scores. Recent work [43] and our empirical analysis (Table 1.1) both show Partial-AUC metrics are more consistent with Top-K accuracy, with the average inconsistency ratio reduced to 21.86%.

Nevertheless, we identify several critical limitations. First, the residual inconsistency between Partial-AUC and Top-K accuracy remains non-negligible. Second, Partial-AUC metrics are highly complex, involving three indicator functions, significantly increasing the optimization difficulty. This complexity manifests in their surrogate loss functions, which often necessitate adversarial training [57], potentially compromising training stability and effectiveness. Our experimental observations confirm the instability of LLPAUC loss (*cf.* Table 3.1), which in some cases underperforms the basic BPR loss. Third, these losses introduce additional hyperparameters (*e.g.*, η_α and η_β in (2.4)), requiring expensive tuning. These limitations heavily hinder the practical applications of these losses.

NDCG@K Surrogate Loss. Recently, a contemporaneous and parallel study, SL@K [58], has been proposed to optimize the Top-K ranking metric NDCG@K. For each user, SL@K is defined as:

$$\mathcal{L}_{\text{SL@}K} = -\frac{1}{|\mathcal{P}_u|} \sum_{i \in \mathcal{P}_u} \left[\sigma\left((s_{ui} - \beta_u^k)/\tau_w\right) \log \sum_{j \in \mathcal{I}} \exp\left((s_{uj} - s_{ui})/\tau\right) \right]$$
(2.5)

where τ_w and τ are two hyperparameters; β_u^k is a user-specific score threshold (the score at rank K); σ is the sigmoid function. SL@K has been shown to serve as an upper bound for NDCG@K [58].

However, several limitations warrant attention: 1) SL@K is designed to optimize NDCG@K, rather than the Top-K accuracy (*e.g.*, Precision@K and Recall@K). These metrics differ substantially. As demonstrated in Table 1.1, NDCG@K exhibits notable inconsistency with Top-K accuracy (20.04% on average). Moreover, Precision@K and Recall@K are more prevalent in industrial RS and align more closely with common online business metrics [8, 10, 35, 65]. 2) SL@K does not provide theoretical guarantees for robustness against distribution shifts, which is essential for RS [53]. 3) SL@K demonstrates instability with fewer negative training signals (*cf.* Table A.2). 4) SL@K relies on Monte-Carlo method to estimate the Top-K threshold, which often incurs a high estimation error (0.18 on average, *cf.* Table A.4). 5) SL@K introduces an extra hyperparameter τ_w that requires exhaustive tuning. These observations motivate the development of loss functions tailored for Top-K accuracy while addressing the aforementioned challenges.

3 Methodology

In this section, we first detail the proposed loss Talos for optimizing Top-K accuracy, and then we conduct comprehensive theoretical analyses to demonstrate its effectiveness.

3.1 Loss Function for Top-K Accuracy

Our Talos first employs a quantile-based approach to simplify the ranking-dependent truncation term. We subsequently design a regression method to enable efficient and accurate threshold estimation, and introduce an additional constraint term to ensure optimization stability. Finally, we integrate a customized surrogate function to mitigate discontinuities and improve distributional robustness.

Introducing Quantile Technique: To tackle the non-feasible ranking-dependent truncation term, we borrow the quantile technique [13, 25, 40]. For each user, we introduce a score threshold named quantile that separates the Top-K items from the rest according to their scores. The formal threshold can be defined as:

$$\beta_u^k = s_{ui}, \text{ where } \pi_{ui} = K$$
(3.1)

which represents the score of the item exactly at the K-th position. When the item score exceeds the threshold, *i.e.*, $s_{ui} \geq \beta_u^k$, it indicates that the item is included in Top-K, while $s_{ui} < \beta_u^k$ implies it does not.

This technique simplifies the complex truncation term $\mathbb{I}(\pi_{ui} \leq K)$ into a simple comparison between item scores and the threshold $\mathbb{I}(s_{ui} \geq \beta_u^k)$, heavily facilitating fast computation and optimization. Specifically, the Precision@K[1] optimization can be transformed as:

$$-\log \text{Precision@}K = -\log \sum_{i \in \mathcal{P}_u} \frac{\mathbb{I}(s_{ui} \geq \beta_u^k)}{K}$$
(3.2)

Here the objective only involves the model-predicted scores and thresholds. However, this quantile-based transformation further raises two challenges: 1) **Threshold estimation**: the Top-K threshold plays a central role in the optimization, and its precise estimation is crucial. Furthermore, the threshold must be computed individually for each user and evolves throughout training, thereby imposing significant computational demands. Conventional regression based strategies [25] are computationally prohibitive in RS, while Monte Carlo-based approaches [58] suffer from considerable estimation bias (*cf.* Table A.4). Consequently, efficient and accurate threshold estimation in RS remains largely underexplored. 2) **Convergence concern**: The evolving threshold also poses risks to optimization convergence. In particular, we observe that directly optimizing Eq.(3.2) often leads to pathological and unstable results, in which both positive and negative item scores, together with the thresholds, iteratively increase in a synchronized manner. This phenomenon, termed score inflation, is not desirable, as RS aim to differentiate positive and negative items and target positioning positive items at the Top-K. How to ensure the stable optimization is also an important question to be addressed.

Efficient Quantile Estimation: Quantile estimation [25] has been well-studied in statistical learning literature. A prominent method is quantile regression [13]. However, estimating Top-K quantile for a user in vanilla quantile regression requires traversing the complete item space (*cf.* Appendix H.1), which is computationally intensive in large-scale RS. To address this, we propose an efficient negative sampling-based quantile regression loss:

$$Q_K(u) = \frac{1}{|\mathcal{I}|} \left(\sum_{i \in \mathcal{P}_u} \rho_K(s_{ui} - \hat{\beta}_u) + w_u \sum_{j \in G_u} \rho_K(s_{uj} - \hat{\beta}_u) \right)$$
(3.3)

where $w_u = \frac{|\mathcal{I}| - |\mathcal{P}_u|}{|G_u|}$, $\rho_K(x) = (1 - K/|\mathcal{I}|)(x)_+ + (K/|\mathcal{I}|)(-x)_+$ with $(x)_+ = \max\{0, x\}$, and G_u denotes the sampled negative item set from $\mathcal{N}_u$. We introduce importance weights w_u to ensure unbiased estimation (*i.e.*, $\mathbb{E}_{G_u}[Q_K(u)] = \mathcal{L}_{\text{QR}}(u)$, *cf.* Appendix H.1 for proof). This treatment can not only reduce the computational complexity to $O(|G_u| + |\mathcal{P}_u|)$ for a user, but remain high estimation accuracy. The estimation error is less than 0.02 as reported in Table A.4.

---

[1] Considering Precision@K may achieve the value 0, making the express $-\log \text{Precision@}K$ ill-defined. For rigor, we extend the support of the function and re-define $\log(x)$ as $\log(0) = \log(\epsilon)$, where ϵ denotes a sufficient small constant.

Constrained Optimization for Stable Convergence: To tackle the inflation issue, we further transform Eq.(3.2) into:

$$\text{Eq.}(3.2) = -\log \frac{\sum_{i \in \mathcal{P}_u} \delta(s_{ui} - \beta_u^k)}{\sum_{j \in \mathcal{I}} \delta(s_{uj} - \beta_u^k)} \tag{3.4}$$

The equality holds due to the fact $\sum_{j \in \mathcal{I}} \mathbb{I}(s_{uj} \geq \beta_u^k) = K$. Here $\delta(x)$ denotes the Heaviside step function with $\delta(x) = \mathbb{I}(x \geq 0)$. The introduction of new denominator could naturally penalize the number of items larger than the Top-K quantile, avoiding the score inflation phenomenon. From a theoretical view, Eq.(3.4) can be understood as an objective equipped with constraint $\log \sum_{j \in \mathcal{I}} \delta(s_{uj} - \beta_u^k) = \log K$. Note that the Lagrange multiplier function of objective Eq.(3.2) with this constraint can be written as follows:

$$-\log \frac{1}{K} \sum_{i \in \mathcal{P}_u} \delta(s_{ui} - \beta_u^k) + \lambda(\log \sum_{j \in \mathcal{I}} \delta(s_{uj} - \beta_u^k) - \log K) \tag{3.5}$$

If we simply set the parameter $\lambda = 1$ and drop the irrelevant constant, we can obtain Eq.(3.4). The introduction of the denominator term helps mitigate the inflation of the score s_{ui}, as it enforces a penalty such that only K items can exceed the quantile threshold. This constraint is crucial, and our empirical results demonstrate significant performance improvements when incorporating this denominator term (*cf.* Table 4.1).

Introducing Customized Surrogate Function: Note that the discontinuity mainly arises from the Heaviside function $\delta(x)$. The conventional solution is to develop a proper activation function to approximate it as $\sigma(\cdot) \approx \delta(\cdot)$. Previous works [18, 19, 58] typically introduce a temperature τ within the sigmoid function $\sigma(\cdot) = \text{sigmoid}(\cdot/\tau)$ to approximate the Heaviside step function. In this work, we incorporate τ outside the sigmoid function, *i.e.*, $\sigma_\tau(\cdot) = \text{sigmoid}(\cdot)^{1/\tau}$ and define our Talos as follows:

$$\mathcal{L}_{\text{Talos}} = -\log \frac{\sum_{i \in \mathcal{P}_u} \sigma_\tau(s_{ui} - \beta_u^k)}{\sum_{j \in \mathcal{I}} \sigma_\tau(s_{uj} - \beta_u^k)} \tag{3.6}$$

This design has multiple advantages: 1) It equips Talos with distributional robustness. In Section 3.2, we demonstrate that optimizing Talos is equivalent to performing distributional robustness optimization, ensuring the model is optimized under distribution perturbations. However, the function with inner temperature cannot enjoy such a merit. 2) This design ensures Talos serving as an tight upper bound for $-\log \text{Precision}@K$ (*cf.* Theorem 3.1), ensuring optimizing Talos can improve Top-K accuracy. 3) Empirical results presented in Table 4.1 also demonstrate that activation with an outside temperature performs much better than inside.

Implementation Details. The optimization process alternates between two steps: 1) updating model parameters through gradient descent using Eq.(3.6); 2) updating quantile estimates via gradient descent using Eq.(3.3). This procedure iterates until convergence. Besides, to address scalability challenges with large item sets, a negative sampling strategy is adopted in the calculation of Talos, similar to SL and LLPAUC, where the denominator term in Eq.(3.6) is computed over a sampled subset of negative items.

Finally, note that Talos involves retrieving all positive items for each user, which may incur implementation complexity and does not facilitate parallel computation. Therefore, in practice, we simply

change the order of the summation and logarithmic operations as:

$$\mathcal{L}_{\text{Talos}} = -\frac{1}{|\mathcal{P}_u|} \sum_{i \in \mathcal{P}_u} \log \frac{\sigma_\tau(s_{ui} - \beta_u^k)}{\sum_{j \in G_u} \sigma_\tau(s_{uj} - \beta_u^k)} \tag{3.7}$$

This formulation greatly facilitates implementation. We do not need to sum over all positive items in the system, which also facilitates mini-batch updates — we can sample a mini-batch of positive items for optimization. In fact, this transformation has a theoretical basis where Eq.(3.4) can be upper bounded by Eq.(3.7) due to the Jensen's inequality [21].

3.2 Analyses on Talos

Our proposed Talos offers several advantages:

Advantage 1: Concise and efficient. Talos has a concise form (*cf.* Eq.(3.7)). Compared to SL, it differs only in integrating the quantile β_u^k and replacing the activation from $\exp(x)^{1/\tau}$ to $\text{sigmoid}(x)^{1/\tau}$. Such a simple revision allows Talos to approximately optimize Top-K accuracy. Similar to SL, only hyperparameter τ is introduced.

Regarding the efficiency, the time complexity of Talos is calculated as $O(\bar{P}|\mathcal{U}||G_u|)$ for both quantile estimation and loss optimization, which is the same as SL. Here, $\bar{P}$ denotes the average number of positive items per user; G_u denotes the sampled negative item set satisfying $|G_u| \ll |\mathcal{I}|$. Our experiments also confirm the computational efficiency of Talos (*cf.* Appendix F).

Advantage 2: Tight surrogate for optimizing Precision@K. We establish theoretical connections between Talos and Precision@K:

THEOREM 3.1 (TALOS SERVES AS A TIGHT SURROGATE FOR PRECISION@K). *For a proper τ, satisfying $\tau \in \left[\frac{\log\left((e^2+2)\,\text{sigmoid}(-2)/2\right)}{\log \epsilon}, \frac{\log(1/2)}{\log \epsilon} \right]$, we have the following bound relations:*

$$-\log \text{Precision}@K \leq \mathcal{L}_{\text{Talos}} + C \tag{3.8}$$

where $C = \log(1 + e^2/2)^{1/\tau}$ is a constant.

The proof is given in Appendix A.1. This theorem ensures that optimizing Talos can lower the upper bound of $-\log \text{Precision}@K$, and thus improve the Precision@K with theoretical guarantee.

Advantage 3: Robustness to distribution shifts. We establish a connection between Talos and the *Distributionally Robustness Optimization* (DRO). Specifically, we have:

THEOREM 3.2 (DISTRIBUTIONAL ROBUSTNESS). *For user u and positive item i, let $\hat{Q}$ be the uniform negative distribution over $\mathcal{N}_u$. Given a robustness radius $\eta > 0$, consider the uncertainty set $\mathbb{Q}$ consisting of all perturbed distributions Q, which is constrained by the KL divergence, i.e., $D_{KL}(Q \| \hat{Q}) \leq \eta$. Let $\sigma(x)$ be a sigmoid function, optimizing Talos is equivalent to solving the following optimization problem:*

$$-\frac{1}{|\mathcal{P}_u|} \sum_{i \in \mathcal{P}_u} \log \sigma(s_{ui} - \beta_u^k) + \max_{Q \in \mathbb{Q}} \mathbb{E}_{j \sim Q} \left[\log \sigma(s_{uj} - \beta_u^k) \right] \tag{3.9}$$

The proof is presented in Appendix A.2. Theorem 3.2 demonstrates Talos is equivalent to performing DRO [52, 53, 62], a theoretically sound tool that empowers models with robustness to distribution shifts. Intuitively, it can be understood that the model is trained not only on the original uniform negative distribution $\hat{Q}$, but across a family of adversarially perturbed distributions. Thus, the model trained under DRO would exhibit robustness. With proper design, our Talos can inherit this property from DRO through equivalence.

Table 3.1: Overall performance comparison of Talos with other losses. blue indicates the best result, and the runner-up is underlined. **Imp.%** indicates the relatively improvements of Talos over the best baselines. "P@20" denotes the metric Precision@20, and "R@20" denotes Recall@20; The mark '*' suggests the improvement is statistically significant with $p < 0.05$.

Model	Loss	Gowalla		Beauty		Games		Electronics	
		P@20	R@20	P@20	R@20	P@20	R@20	P@20	R@20
MF	BPR	0.0438	0.1511	0.0146	0.1267	0.0142	0.1334	0.0058	0.0566
	AATP	0.0327	0.1078	0.0120	0.1044	0.0142	0.1330	0.0028	0.0272
	RS@K	0.0397	0.1218	0.0094	0.0669	0.0104	0.0872	0.0020	0.0159
	SmoothI@K	0.0586	0.1882	0.0163	0.1352	0.0192	0.1778	0.0059	0.0565
	SL	0.0625	0.2017	0.0172	0.1403	0.0208	0.1918	0.0064	0.0626
	BSL	0.0625	0.2017	0.0171	0.1401	<u>0.0210</u>	0.1934	0.0065	0.0630
	PSL	<u>0.0631</u>	<u>0.2031</u>	<u>0.0174</u>	<u>0.1432</u>	<u>0.0210</u>	0.1935	<u>0.0066</u>	<u>0.0637</u>
	AdvInfoNCE	0.0623	0.2012	0.0171	0.1403	<u>0.0210</u>	<u>0.1935</u>	0.0063	0.0616
	LLPAUC	0.0562	0.1847	0.0157	0.1336	0.0187	0.1748	0.0059	0.0583
	Talos	**0.0642**	**0.2079**	**0.0179**	**0.1499**	**0.0213**	**0.1967**	**0.0067**	**0.0655**
	Imp.%	**+1.71%***	**+2.35%***	**+2.69%***	**+4.69%***	**+1.19%***	**+1.62%***	**+3.04%***	**+2.75%***
LGCN	BPR	0.0527	0.1761	0.0159	0.1385	0.0192	0.1801	0.0050	0.0482
	AATP	0.0249	0.0754	0.0121	0.1067	0.0127	0.1175	0.0030	0.0289
	RS@K	0.0536	0.1735	0.0151	0.1192	0.0168	0.1511	0.0038	0.0357
	SmoothI@K	0.0590	0.1898	0.0169	0.1427	0.0196	0.1801	0.0065	0.0630
	SL	0.0628	0.2025	0.0172	<u>0.1433</u>	<u>0.0211</u>	<u>0.1942</u>	0.0065	0.0629
	BSL	0.0628	0.2025	0.0172	0.1433	0.0210	0.1931	0.0064	0.0626
	PSL	<u>0.0634</u>	<u>0.2042</u>	<u>0.0173</u>	0.1425	0.0210	0.1925	0.0065	0.0627
	AdvInfoNCE	0.0627	0.2028	0.0172	0.1433	0.0210	0.1936	0.0064	0.0626
	LLPAUC	0.0516	0.1722	0.0170	0.1423	0.0202	0.1882	<u>0.0066</u>	<u>0.0642</u>
	Talos	**0.0642**	**0.2080**	**0.0178**	**0.1489**	**0.0212**	**0.1960**	**0.0068**	**0.0662**
	Imp.%	**+1.26%***	**+1.85%***	**+3.08%***	**+3.87%***	**+0.68%***	**+0.95%***	**+3.48%***	**+3.06%***
XSimGCL	BPR	0.0584	0.1917	0.0170	<u>0.1450</u>	0.0194	0.1810	0.0064	0.0625
	AATP	0.0451	0.1515	0.0153	0.1264	0.0173	0.1619	0.0051	0.0501
	RS@K	0.0515	0.1669	0.0151	0.1221	0.0174	0.1590	0.0040	0.0373
	SmoothI@K	0.0532	0.1731	0.0077	0.0560	0.0144	0.1320	0.0040	0.0395
	SL	0.0623	0.2010	0.0171	0.1418	0.0208	0.1915	0.0065	0.0627
	BSL	0.0625	0.2013	0.0169	0.1413	<u>0.0209</u>	<u>0.1931</u>	0.0063	0.0619
	PSL	<u>0.0630</u>	<u>0.2023</u>	<u>0.0172</u>	0.1407	0.0207	0.1910	<u>0.0066</u>	<u>0.0636</u>
	AdvInfoNCE	0.0623	0.2010	0.0171	0.1415	0.0209	0.1923	0.0064	0.0622
	LLPAUC	0.0612	0.1980	0.0171	0.1443	0.0207	0.1910	0.0064	0.0635
	Talos	**0.0638**	**0.2057**	**0.0180**	**0.1506**	**0.0212**	**0.1961**	**0.0067**	**0.0654**
	Imp.%	**+1.27%***	**+1.68%***	**+4.87%***	**+3.81%***	**+1.32%***	**+1.60%***	**+2.65%***	**+2.81%***

Advantage 4: Convergence Guarantee. While the proposed optimization process involves dynamic update between Eq.(3.3) and Eq.(3.6), it has the following theoretical convergence guarantee:

THEOREM 3.3 (CONVERGENCE GUARANTEE). *Let K be the Lipschitz constant of $\mathcal{L}_{Talos}$. With the fixed stepsize $0 < \alpha < 2/K$, the gradient norm is bounded by:*

$$\frac{(2\alpha - K\alpha^2)}{4} \mathbb{E}_t \left[\| \nabla \mathcal{L}_{Talos}^{(t)} \|^2 \right] \leq \frac{1}{T} \mathcal{L}_{Talos}^{(0)} \tag{3.10}$$

where T denotes the total number of optimization iterations, $\nabla \mathcal{L}_{Talos}^{(t)}$ denotes the gradient of the loss w.r.t. the score variables at iteration t, and $\mathcal{L}_{Talos}^{(0)}$ denotes the the initial loss value.

The proof is presented in Appendix A.3. Theorem 3.3 provides a theoretical foundation for Talos optimization reliability.

4 Experiments

4.1 Experimental Setup

Recommendation Backbones. We closely refer to Yang et al. [57] and evaluate Talos and baselines on three distinct recommendation backbones: the classic Matrix Factorization (MF) model [38], the representative graph-based model LightGCN [16], and the SOTA method XSimGCL [59]. See Appendix D.2 for more details.

Baselines. The following baselines are included: 1) **BPR** [38], the classic pair-wise loss in RS; 2) **SL** [54]: the loss approximately optimizing the NDCG; 3) **BSL** [53], **AdvInfoNCE** [61], and **PSL** [57]: three enhanced variants of SL from different perspectives, achieving SOTA performance; 4) **LLPAUC** [43], the loss approximately optimizing the lower-left partial AUC; 5) **SmoothI@**K [46], **RS@**K [34], and **AATP** [2], three surrogate losses for Top-K metrics. Note that

Table 3.2: Performance comparisons with varying *K* on MF backbone in Gowalla dataset. blue **indicates the best result.**

Gowalla	Recall@20	Recall@50	Recall@80
AATP	0.1062	0.2068	0.2160
RS@*K*	0.1218	0.1059	0.2406
SmoothI@*K*	0.1882	0.3027	0.3625
SL	0.2017	0.3185	0.3900
BSL	0.2017	0.3185	0.3900
AdvInfoNCE	0.2013	0.3183	0.3900
LLPAUC	0.1847	0.2927	0.3640
PSL	0.2038	0.3192	0.3902
Talos@20	**0.2078**	0.3202	0.3894
Talos@50	0.2078	**0.3212**	0.3907
Talos@80	0.2074	0.3211	**0.3911**
Imp.%	**+1.98%**	**+0.63%**	**+0.22%**

Table 3.3: Performance comparisons with varying *K* on MF backbone in Beauty dataset. blue **indicates the best result.**

Beauty	Recall@20	Recall@50	Recall@80
AATP	0.1077	0.1850	0.2371
RS@*K*	0.0669	0.0989	0.1223
SmoothI@*K*	0.1352	0.2041	0.2454
SL	0.1403	0.2163	0.2617
BSL	0.1401	0.2159	0.2617
AdvInfoNCE	0.1409	0.2160	0.2621
LLPAUC	0.1336	0.2047	0.2443
PSL	0.1432	0.2184	0.2625
Talos@20	**0.1499**	0.2205	0.2620
Talos@50	0.1484	**0.2218**	0.2637
Talos@80	0.1485	0.2213	**0.2674**
Imp.%	**+1.85%**	**+4.69%**	**+1.59%**

Table 3.4: Temporal shift explorations. P@20 denotes Precision@20, while R@20 denotes Recall@20.

Dataset	Metric	AATP	RS@*K*	SmoothI@*K*	SL	BSL	PSL	AdvInfoNCE	LLPAUC	Talos	Imp.%
Gowalla	**P@20**	0.0300	0.0404	0.0544	0.0544	0.0544	0.0542	0.0542	0.0567	**0.0574**	**+1.24%**
	R@20	0.0807	0.1103	0.1497	0.1497	0.1497	0.1492	0.1499	0.1541	**0.1577**	**+2.37%**
Beauty	**P@20**	0.0061	0.0046	0.0076	0.0089	0.0089	0.0086	0.0089	0.0087	**0.0094**	**+5.51%**
	R@20	0.0461	0.0381	0.0589	0.0696	0.0697	0.0679	0.0699	0.0697	**0.0738**	**+5.45%**

these methods are tailored for other domains, and their effectiveness in RS is limited. We discuss these methods in Section 5.

Datasets. We conduct experiments on four widely-used datasets containing users' ratings on items: **Beauty**, **Games**, **Electronics** [57] and **Gowalla** [16]. See Appendix D.3 for more details.

Hyperparameter Setting. A grid search is adopted to find optimal hyperparameters. For all compared methods, we closely follow configurations in their respective publications to ensure the optimal performance. We refer readers to Appendix D.5 for more details.

4.2 Analysis on Experiment Details

Talos VS. others. Table 3.1 compares Talos with other baselines. Overall, Talos outperforms all baselines across all datasets and backbones. Especially in Beauty, Talos achieves the impressive improvements — 3.83% average on two evaluation metrics, highlighting the effectiveness of Talos that directly optimizes Top-*K* accuracy. Additional results in Appendix E demonstrate Talos also brings improvements on NDCG@*K* and MRR@*K*.

LLPAUC VS. SL. While LLPAUC demonstrates a stronger correlation with Top-*K* metrics than SL, we observe it does not consistently outperforms SL. In fact, LLPAUC is unstable across different backbones, even worse than basic BPR on Gowalla with LGCN.
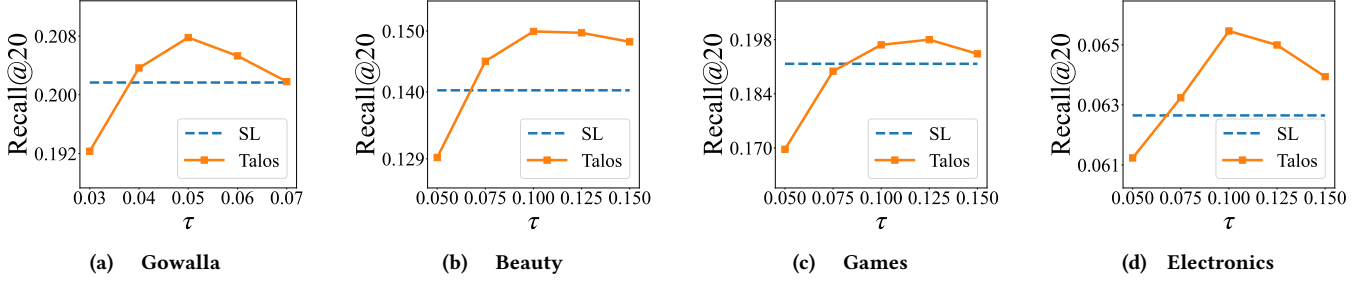
Performance comparison with varying *K*. Tables 3.2 and 3.3 illustrate the performance across different values of *K*. We observe that Talos consistently outperforms the compared methods for various *K* values. However, as *K* increases, the magnitude of the improvements decreases. This observation aligns with our intuition. As *K* increases, the Top-*K* accuracy gradually degrades to the full ranking metrics. Consequently, the advantage of optimizing for Top-*K* accuracy diminishes as *K* grows.

Consistency study. Tables 3.2 and 3.3 present Recall@*K'*, and the performance of Talos@*K* for varying values $K, K' \in \{20, 50, 80\}$. We

observe that the best performance is achieved when $K = K'$, aligned with our expectations. For instance, when evaluating Recall@80 for a model trained with Talos@20 (targets optimizing for Recall@20), the discrepancy between *K* and *K'* leads to performance drop.

Performance with distribution shifts. To evaluate the robustness against distribution shifts, we follow [47], introducing temporal bias to construct the test scenario with distribution shifts (*cf.* Appendix D.4). Table 3.4 shows that Talos achieves the best performance, demonstrating its superior distributional robustness. LLPAUC benefits from adversarial training and exhibits fine robustness. Moreover, Talos achieves more pronounced average improvements than in IID setting, *i.e.*, 1.26% → 3.37%. The effectiveness can be attributed to its connection with DRO.

Ablation study. In Table 4.1, we evaluate three Talos variants: 1) quantile fixed as zero (w/o-quantile); 2) sigmoid$(\cdot)^{1/\tau}$ replaced by sigmoid$(\cdot/\tau)$ (w/o-outside); 3) the denominator term in Eq.(3.6) replaced by the constant *K* (w/o-denominator). Talos outperforms all variants. We highlight three key observations: 1) The gap between Talos and w/o-quantile highlights the importance of quantile technique; 2) Talos surpasses w/o-outside, indicating the superiority of introducing DRO; 3) Compared to w/o-denominator, results confirm our analysis in Section 3.1 that Talos naturally penalizes negatives exceeding the Top-*K* quantile, addressing score inflation.

Temperature Sensitivity. Figure 2 depicts the performance with varying τ in Talos. Performance initially improves as τ increases, but degrades beyond a certain point. This aligns with Theorem 3.1: When τ satisfies the surrogate condition, smaller τ means the tighter upper bound for Top-*K* accuracy but increases training difficulty due to the decreased Lipschitz smoothness. As τ increases, the approximation would be looser, even not satisfy the surrogate condition, thus impacting performance.

Figure 2: Sensitivity analysis of Talos on τ, where - - - denotes the performance of SL with optimal hyperparameter.

| (a) Gowalla | (b) Beauty | (c) Games | (d) Electronics |

Table 4.1: Ablation study, we examine three variations of Talos, where the quantile is removed (w/o-quantile), the sigmoid$(x)^{1/\tau}$ form is replaced by sigmoid(x/τ) (w/o-outside), and the denominator term is replaced by the constant K (w/o-denominator).

Loss	Gowalla		Beauty		Games		Electronics	
	Precision@20	Recall@20	Precision@20	Recall@20	Precision@20	Recall@20	Precision@20	Recall@20
w/o-quantile	0.0626	0.2037	0.0175	0.1487	0.0208	0.1931	0.0066	0.0640
w/o-outside	0.0577	0.1859	0.0166	0.1375	0.0194	0.1799	0.0062	0.0592
w/o-denominator	0.0278	0.0869	0.0101	0.0841	0.0127	0.1173	0.0018	0.0160
Talos	**0.0642**	**0.2079**	**0.0179**	**0.1499**	**0.0213**	**0.1967**	**0.0067**	**0.0655**

5 Related Work

Since this work focuses on recommendation loss functions, here we mainly introduce related work on this topic. For the area of recommendation models and recommendation loss consistency, we refer readers to Appendix C. In recommendation losses, two prominent types stand out: 1) full ranking optimization losses such as BPR [38] and SL [54]. BPR optimizes the relative ranking of positive items over negatives as an AUC surrogate, while SL has been shown to approximately optimize the NDCG ranking metric with excellent performance. Motivated by the success of SL, several works attempted to improve it: BSL [53] and AdvInfoNCE [61] introduced the DRO framework to enhance SL's robustness. PSL [57] replaced the exponential function in SL with other appropriate activation functions, serving as a tighter surrogate for NDCG. 2) LLPAUC [43], which evaluates the lower left part of AUC, demonstrates a strong correlation with Top-K accuracy. Beyond these two types, recent works explored alternative losses [28, 41], but these do not optimize Top-K accuracy.

Notably, Top-K optimization has also been investigated in other fields, yet these approaches fall short when applied to RS. For instance, AATP [2] serves as a surrogate Top-K loss by integrating quantile. Nevertheless, this loss is heuristically designed, which lacks theoretical connections to Top-K accuracy. Furthermore, it fails to address the common distribution shifts in RS (cf. Table 3.4). In image retrieval, Pre@K [31] and RS@K [34] optimize Precision@K and Recall@K, respectively. However, they either integrated the complicated sampling strategy or rely on nested approximations of both ranking positions and indicator functions, which exacerbate errors when aligning with Top-K accuracy. In information retrieval, SmoothI@K [46] employs the softmax function to approximate Top-K indicators through a complex recursive estimation process, leading to inaccurate approximations particularly in RS with large item sets. As shown in Table 3.1, SmoothI@K underperforms even the basic BPR when applied with the XSimGCL backbone.

Recently, a contemporaneous and parallel study, SL@K [58], focuses on optimizing NDCG@K. We emphasize that Talos differs

from SL@K in several important aspects: 1) This work targets the optimization of Precision@K and Recall@K, whereas SL@K is designed to optimize NDCG@K. These metrics are not consistent as discussed in Section 2.3. 2) Talos demonstrates the robustness to distribution shifts, while SL@K does not. Under temporal shifts, Talos achieves superior performance (over 1.12%, cf. Table A.1). 3) Talos achieves greater stability when fewer negative items are sampled, yielding markedly higher performance compared with SL@K (over 1.96%, cf. Table A.2). 4) Talos incorporates a more accurate threshold estimation strategy, resulting in substantially lower estimation error than SL@K (0.01 v.s. 0.18, cf. Table A.4). 5) SL@K requires a greater number of hyperparameters, considerably limiting its practicality.

6 Conclusion and Future Works

This work introduces Talos, tailored for optimizing Top-K accuracy in recommender systems. Talos incorporates an efficient quantile-based technique to handle the ranking-dependent challenge; introduces a constraint optimization term to address the score inflation issue; and leverage a specific surrogate function to tackle the discontinuity problem, equipping the loss with distributional robustness. Our theoretical analysis confirms the close bounded relationship between Precision@K and Talos, equivalence to distributionally robustness optimization, and convergence guarantees. Beyond these strengths, Talos is concise in form and computationally efficient, making it practical in RS. Considering Talos still introduces a temperature hyperparameter, developing adaptive τ mechanisms such as connecting τ to the number of positive interactions or using meta-learning, is a promising direction for future research.

Acknowledgments

References

[1] Robert Bell, Yehuda Koren, and Chris Volinsky. 2007. Modeling relationships at multiple scales to improve accuracy of large recommender systems. In *Proceedings of the 13th ACM SIGKDD international conference on Knowledge discovery and data mining*. 95–104.

[2] Stephen Boyd, Corinna Cortes, Mehryar Mohri, and Ana Radovanovic. 2012. Accuracy at the top. *Advances in neural information processing systems* 25 (2012).

[3] Jiawei Chen, Hande Dong, Yang Qiu, Xiangnan He, Xin Xin, Liang Chen, Guli Lin, and Keping Yang. 2021. AutoDebias: Learning to debias for recommendation. In *Proceedings of the 44th International ACM SIGIR Conference on Research and Development in Information Retrieval*. 21–30.

[4] Jiawei Chen, Hande Dong, Xiang Wang, Fuli Feng, Meng Wang, and Xiangnan He. 2023. Bias and debias in recommender system: A survey and future directions. *ACM Transactions on Information Systems* 41, 3 (2023), 1–39.

[5] Jiawei Chen, Junkang Wu, Jiancan Wu, Xuezhi Cao, Sheng Zhou, and Xiangnan He. 2023. Adap-τ: Adaptively modulating embedding magnitude for recommendation. In *Proceedings of the ACM Web Conference 2023*. 1085–1096.

[6] Sirui Chen, Jiawei Chen, Sheng Zhou, Bohao Wang, Shen Han, Chanfei Su, Yuqing Yuan, and Can Wang. 2024. SIGformer: Sign-aware graph transformer for recommendation. In *Proceedings of the 47th international ACM SIGIR conference on research and development in information retrieval*. 1274–1284.

[7] Sirui Chen, Shen Han, Jiawei Chen, Binbin Hu, Sheng Zhou, Gang Wang, Yan Feng, Chun Chen, and Can Wang. 2025. Rankformer: A Graph Transformer for Recommendation based on Ranking Objective. In *Proceedings of the ACM on Web Conference 2025*. 3037–3048.

[8] Paul Covington, Jay Adams, and Emre Sargin. 2016. Deep neural networks for youtube recommendations. In *Proceedings of the 10th ACM conference on recommender systems*. 191–198.

[9] Yu Cui, Feng Liu, Jiawei Chen, Canghong Jin, Xingyu Lou, Changwang Zhang, Jun Wang, Yuegang Sun, and Can Wang. 2025. HatLLM: Hierarchical Attention Masking for Enhanced Collaborative Modeling in LLM-based Recommendation. *arXiv preprint arXiv:2510.10955* (2025).

[10] Yu Cui, Feng Liu, Jiawei Chen, Xingyu Lou, Changwang Zhang, Jun Wang, Yuegang Sun, Xiaohu Yang, and Can Wang. 2025. Field Matters: A lightweight LLM-enhanced Method for CTR Prediction. *arXiv preprint arXiv:2505.14057* (2025).

[11] Yu Cui, Feng Liu, Pengbo Wang, Bohao Wang, Heng Tang, Yi Wan, Jun Wang, and Jiawei Chen. 2024. Distillation matters: empowering sequential recommenders to match the performance of large language models. In *Proceedings of the 18th ACM Conference on Recommender Systems*. 507–517.

[12] Chongming Gao, Kexin Huang, Jiawei Chen, Yuan Zhang, Biao Li, Peng Jiang, Shiqi Wang, Zhong Zhang, and Xiangnan He. 2023. Alleviating matthew effect of offline reinforcement learning in interactive recommendation. In *Proceedings of the 46th International ACM SIGIR Conference on Research and Development in Information Retrieval*. 238–248.

[13] Lingxin Hao and Daniel Q Naiman. 2007. *Quantile regression*. Number 149. Sage.

[14] F Maxwell Harper and Joseph A Konstan. 2015. The movielens datasets: History and context. *Acm transactions on interactive intelligent systems (tiis)* 5, 4 (2015), 1–19.

[15] Ruining He and Julian McAuley. 2016. VBPR: visual bayesian personalized ranking from implicit feedback. In *Proceedings of the AAAI conference on artificial intelligence*, Vol. 30.

[16] Xiangnan He, Kuan Deng, Xiang Wang, Yan Li, Yongdong Zhang, and Meng Wang. 2020. LightGCN: Simplifying and powering graph convolution network for recommendation. In *Proceedings of the 43rd International ACM SIGIR conference on research and development in Information Retrieval*. 639–648.

[17] Xiangnan He, Lizi Liao, Hanwang Zhang, Liqiang Nie, Xia Hu, and Tat-Seng Chua. 2017. Neural collaborative filtering. In *Proceedings of the 26th international conference on world wide web*. 173–182.

[18] A Iliev, Nikolay Kyurkchiev, and Svetoslav Markov. 2017. On the approximation of the step function by some sigmoid functions. *Mathematics and Computers in Simulation* 133 (2017), 223–234.

[19] Anton Iliev Iliev, Nikolay Kyurkchiev, and Svetoslav Markov. 2015. On the approximation of the cut and step functions by logistic and Gompertz functions. *Biomath* 4, 2 (2015), ID–1510101.

[20] Ashish Jaiswal, Ashwin Ramesh Babu, Mohammad Zaki Zadeh, Debapriya Banerjee, and Fillia Makedon. 2020. A survey on contrastive self-supervised learning. *Technologies* 9, 1 (2020), 2.

[21] Johan Ludwig William Valdemar Jensen. 1906. Sur les fonctions convexes et les inégalités entre les valeurs moyennes. *Acta mathematica* 30, 1 (1906), 175–193.

[22] Christopher C Johnson et al. 2014. Logistic matrix factorization for implicit feedback data. *Advances in Neural Information Processing Systems* 27, 78 (2014), 1–9.

[23] Diederik P Kingma and Jimmy Ba. 2014. Adam: A method for stochastic optimization. *arXiv preprint arXiv:1412.6980* (2014).

[24] Hyeyoung Ko, Suyeon Lee, Yoonseo Park, and Anna Choi. 2022. A survey of recommendation systems: recommendation models, techniques, and application

[25] R Koenker. 2005. Quantile Regression Cambridge, UK: Cambridge Univ.

[26] Yehuda Koren, Robert Bell, and Chris Volinsky. 2009. Matrix factorization techniques for recommender systems. *Computer* 42, 8 (2009), 30–37.

[27] Siyi Lin, Chongming Gao, Jiawei Chen, Sheng Zhou, Binbin Hu, Yan Feng, Chun Chen, and Can Wang. 2025. How do recommendation models amplify popularity bias? An analysis from the spectral perspective. In *Proceedings of the Eighteenth ACM International Conference on Web Search and Data Mining*. 659–668.

[28] Zhutian Lin, Junwei Pan, Shangyu Zhang, Ximei Wang, Xi Xiao, Shudong Huang, Lei Xiao, and Jie Jiang. 2024. Understanding the ranking loss for recommendation with sparse user feedback. In *Proceedings of the 30th ACM SIGKDD Conference on Knowledge Discovery and Data Mining*. 5409–5418.

[29] Xiao Liu, Fanjin Zhang, Zhenyu Hou, Li Mian, Zhaoyu Wang, Jing Zhang, and Jie Tang. 2021. Self-supervised learning: Generative or contrastive. *IEEE transactions on knowledge and data engineering* 35, 1 (2021), 857–876.

[30] Phil Long and Rocco Servedio. 2013. Consistency versus realizable H-consistency for multiclass classification. In *International conference on machine learning*. PMLR, 801–809.

[31] Jing Lu, Chaofan Xu, Wei Zhang, Ling-Yu Duan, and Tao Mei. 2019. Sampling wisely: Deep image embedding by top-k precision optimization. In *Proceedings of the IEEE/CVF International Conference on Computer Vision*. 7961–7970.

[32] Aaron van den Oord, Yazhe Li, and Oriol Vinyals. 2018. Representation learning with contrastive predictive coding. *arXiv preprint arXiv:1807.03748* (2018).

[33] Rong Pan, Yunhong Zhou, Bin Cao, Nathan N Liu, Rajan Lukose, Martin Scholz, and Qiang Yang. 2008. One-class collaborative filtering. In *2008 Eighth IEEE international conference on data mining*. IEEE, 502–511.

[34] Yash Patel, Giorgos Tolias, and Jiří Matas. 2022. Recall@ k surrogate loss with large batches and similarity mixup. In *Proceedings of the IEEE/CVF Conference on Computer Vision and Pattern Recognition*. 7502–7511.

[35] Qi Pi, Guorui Zhou, Yujing Zhang, Zhe Wang, Lejian Ren, Ying Fan, Xiaoqiang Zhu, and Kun Gai. 2020. Search-based user interest modeling with lifelong sequential behavior data for click-through rate prediction. In *Proceedings of the 29th ACM International Conference on Information & Knowledge Management*. 2685–2692.

[36] Yuanhao Pu, Defu Lian, Xiaolong Chen, Jin Chen, Ze Liu, and Enhong Chen. 2025. Understanding the Effect of Loss Functions on the Generalization of Recommendations. In *Proceedings of the 31st ACM SIGKDD Conference on Knowledge Discovery and Data Mining V. 1*. 1127–1137.

[37] Zhaochun Ren, Xiangnan He, Dawei Yin, Maarten de Rijke, et al. 2024. Information Discovery in E-commerce. *Foundations and Trends® in Information Retrieval* 18, 4-5 (2024), 417–690.

[38] Steffen Rendle, Christoph Freudenthaler, Zeno Gantner, and Lars Schmidt-Thieme. 2009. BPR: Bayesian personalized ranking from implicit feedback. In *Proceedings of the Twenty-Fifth Conference on Uncertainty in Artificial Intelligence*. 452–461.

[39] R Tyrrell Rockafellar and Roger JB Wets. 1998. *Variational analysis*. Springer.

[40] Jun Shao. 2008. *Mathematical statistics*. Springer Science & Business Media.

[41] Xiang-Rong Sheng, Jingyue Gao, Yueyao Cheng, Siran Yang, Shuguang Han, Hongbo Deng, Yuning Jiang, Jian Xu, and Bo Zheng. 2023. Joint optimization of ranking and calibration with contextualized hybrid model. In *Proceedings of the 29th ACM SIGKDD Conference on Knowledge Discovery and Data Mining*. 4813–4822.

[42] Wentao Shi, Jiawei Chen, Fuli Feng, Jizhi Zhang, Junkang Wu, Chongming Gao, and Xiangnan He. 2023. On the theories behind hard negative sampling for recommendation. In *Proceedings of the ACM Web Conference 2023*. 812–822.

[43] Wentao Shi, Chenxu Wang, Fuli Feng, Yang Zhang, Wenjie Wang, Junkang Wu, and Xiangnan He. 2024. Lower-Left Partial AUC: An Effective and Efficient Optimization Metric for Recommendation. In *Proceedings of the ACM on Web Conference 2024*. 3253–3264.

[44] Yue Shi, Martha Larson, and Alan Hanjalic. 2014. Collaborative filtering beyond the user-item matrix: A survey of the state of the art and future challenges. *ACM Computing Surveys (CSUR)* 47, 1 (2014), 1–45.

[45] Xiaoyuan Su and Taghi M Khoshgoftaar. 2009. A survey of collaborative filtering techniques. *Advances in artificial intelligence* 2009, 1 (2009), 421425.

[46] Thibaut Thonet, Yagmur Gizem Cinar, Eric Gaussier, Minghan Li, and Jean-Michel Renders. 2022. Listwise learning to rank based on approximate rank indicators. In *Proceedings of the AAAI Conference on Artificial Intelligence*, Vol. 36. 8494–8502.

[47] Bohao Wang, Jiawei Chen, Changdong Li, Sheng Zhou, Qihao Shi, Yang Gao, Yan Feng, Chun Chen, and Can Wang. 2024. Distributionally Robust Graph-based Recommendation System. In *Proceedings of the ACM on Web Conference 2024*. 3777–3788.

[48] Bohao Wang, Feng Liu, Jiawei Chen, Xingyu Lou, Changwang Zhang, Jun Wang, Yuegang Sun, Yan Feng, Chun Chen, and Can Wang. 2025. Msl: Not all tokens are what you need for tuning llm as a recommender. In *Proceedings of the 48th International ACM SIGIR Conference on Research and Development in Information Retrieval*. 1912–1922.

[49] Bohao Wang, Feng Liu, Changwang Zhang, Jiawei Chen, Yudi Wu, Sheng Zhou, Xingyu Lou, Jun Wang, Yan Feng, Chun Chen, et al. 2025. Llm4dsr: Leveraging

large language model for denoising sequential recommendation. *ACM Transactions on Information Systems* 44, 1 (2025), 1–32.

[50] Wenjie Wang, Xinyu Lin, Fuli Feng, Xiangnan He, Min Lin, and Tat-Seng Chua. 2022. Causal representation learning for out-of-distribution recommendation. In *Proceedings of the ACM Web Conference 2022.* 3562–3571.

[51] Xiang Wang, Xiangnan He, Meng Wang, Fuli Feng, and Tat-Seng Chua. 2019. Neural graph collaborative filtering. In *Proceedings of the 42nd international ACM SIGIR conference on Research and development in Information Retrieval.* 165–174.

[52] Junkang Wu, Jiawei Chen, Jiancan Wu, Wentao Shi, Xiang Wang, and Xiangnan He. 2023. Understanding contrastive learning via distributionally robust optimization. *Advances in Neural Information Processing Systems* 36 (2023), 23297–23320.

[53] Junkang Wu, Jiawei Chen, Jiancan Wu, Wentao Shi, Jizhi Zhang, and Xiang Wang. 2024. Bsl: Understanding and improving softmax loss for recommendation. In *2024 IEEE 40th International Conference on Data Engineering (ICDE).* IEEE, 816–830.

[54] Jiancan Wu, Xiang Wang, Xingyu Gao, Jiawei Chen, Hongcheng Fu, and Tianyu Qiu. 2024. On the effectiveness of sampled softmax loss for item recommendation. *ACM Transactions on Information Systems* 42, 4 (2024), 1–26.

[55] Shiwen Wu, Fei Sun, Wentao Zhang, Xu Xie, and Bin Cui. 2022. Graph neural networks in recommender systems: a survey. *Comput. Surveys* 55, 5 (2022), 1–37.

[56] Marek Wydmuch, Kalina Jasinska, Mikhail Kuznetsov, R'obert Busa-Fekete, and Krzysztof Dembczynski. 2018. A no-regret generalization of hierarchical softmax to extreme multi-label classification. *Advances in neural information processing systems* 31 (2018).

[57] Weiqin Yang, Jiawei Chen, Xin Xin, Sheng Zhou, Binbin Hu, Yan Feng, Chun Chen, and Can Wang. 2024. PSL: Rethinking and Improving Softmax Loss from Pairwise Perspective for Recommendation. *Advances in Neural Information Processing Systems* 37 (2024), 120974–121006.

[58] Weiqin Yang, Jiawei Chen, Shengjia Zhang, Peng Wu, Yuegang Sun, Yan Feng, Chun Chen, and Can Wang. 2025. Breaking the Top-K Barrier: Advancing Top-K Ranking Metrics Optimization in Recommender Systems. In *Proceedings of the 31st ACM SIGKDD Conference on Knowledge Discovery and Data Mining V. 2.* 3542–3552.

[59] Junliang Yu, Xin Xia, Tong Chen, Lizhen Cui, Nguyen Quoc Viet Hung, and Hongzhi Yin. 2023. XSimGCL: Towards extremely simple graph contrastive learning for recommendation. *IEEE Transactions on Knowledge and Data Engineering* 36, 2 (2023), 913–926.

[60] Wenhui Yu and Zheng Qin. 2020. Graph convolutional network for recommendation with low-pass collaborative filters. In *International Conference on Machine Learning.* PMLR, 10936–10945.

[61] An Zhang, Leheng Sheng, Zhibo Cai, Xiang Wang, and Tat-Seng Chua. 2024. Empowering collaborative filtering with principled adversarial contrastive loss. *Advances in Neural Information Processing Systems* 36 (2024).

[62] Shengjia Zhang, Jiawei Chen, Changdong Li, Sheng Zhou, Qihao Shi, Yan Feng, Chun Chen, and Can Wang. 2025. Advancing Loss Functions in Recommender Systems: A Comparative Study with a Rényi Divergence-Based Solution. In *Proceedings of the AAAI Conference on Artificial Intelligence*, Vol. 39. 13286–13294.

[63] Shuai Zhang, Huoyu Liu, Aston Zhang, Yue Hu, Ce Zhang, Yumeng Li, Tanchao Zhu, Shaojian He, and Wenwu Ou. 2021. Learning user representations with hypercuboids for recommender systems. In *Proceedings of the 14th ACM international conference on web search and data mining.* 716–724.

[64] Shuai Zhang, Lina Yao, Aixin Sun, and Yi Tay. 2019. Deep learning based recommender system: A survey and new perspectives. *ACM computing surveys (CSUR)* 52, 1 (2019), 1–38.

[65] Guorui Zhou, Xiaoqiang Zhu, Chenru Song, Ying Fan, Han Zhu, Xiao Ma, Yanghui Yan, Junqi Jin, Han Li, and Kun Gai. 2018. Deep interest network for click-through rate prediction. In *Proceedings of the 24th ACM SIGKDD international conference on knowledge discovery & data mining.* 1059–1068.

[66] Huachi Zhou, Hao Chen, Junnan Dong, Daochen Zha, Chuang Zhou, and Xiao Huang. 2023. Adaptive popularity debiasing aggregator for graph collaborative filtering. In *Proceedings of the 46th International ACM SIGIR Conference on Research and Development in Information Retrieval.* 7–17.

[67] Dixian Zhu, Gang Li, Bokun Wang, Xiaodong Wu, and Tianbao Yang. 2022. When auc meets dro: Optimizing partial auc for deep learning with non-convex convergence guarantee. In *International Conference on Machine Learning.* PMLR, 27548–27573.

[68] Ziwei Zhu, Jianling Wang, and James Caverlee. 2019. Improving top-k recommendation via jointcollaborative autoencoders. In *The World Wide Web Conference.* 3483–3482.

A Theoretical Proofs

A.1 Proof of Theorem 3.1

To prove Theorem 3.1, we first derive Eq.(3.4) as:

$$-\log\text{Precision@}K = \log\sum\nolimits_{j\in\mathcal{I}}\delta(s_{uj}-\beta_u^k) - \log\sum\nolimits_{j\in\mathcal{P}_u}\delta(s_{ui}-\beta_u^k) \tag{A.1}$$

We simplify notation $\delta(s_{ui}-\beta_u^k)$ and $\delta(s_{uj}-\beta_u^k)$ as $\delta(x)$. Here, we simply consider $s_{ui}\in[-1,1]$ and $x\in[-2,2]$ following recent work [53, 57], as cosine similarity is commonly used to generate recommendation. Also, the normalization of prediction values has been demonstrated essential for RS [5]. By selecting $\sigma(x)=\text{sigmoid}(x)^{1/\tau}$, for $\tau\geq\frac{\log\left((e^2+2)\text{sigmoid}(-2)/2\right)}{\log\epsilon}$, the red term can be bounded up as:

$$\begin{cases}\log\delta(x) = \log(\epsilon)\leq\log\sigma(x)+\log(1+e^2/2)^{1/\tau} & ,x\in[-2,0]\\ \log\delta(x)\leq\log(1)^{1/\tau}\leq\log\sigma(x)+\log(1+e^2/2)^{1/\tau} & ,x\in(0,2]\end{cases} \tag{A.2}$$

For τ satisfying $\tau\leq\frac{\log(1/2)}{\log\epsilon}$, the blue term can be bounded up as:

$$\begin{cases}\log\sigma(x)\leq\log(1/2)^{1/\tau}\leq\log\delta(x) & ,x\in[-2,0]\\ \log\sigma(x)\leq\log(1)=\log\delta(x) & ,x\in(0,2]\end{cases} \tag{A.3}$$

Thus, select a proper $\tau\in[\frac{\log\left((e^2+2)\text{sigmoid}(-2)/2\right)}{\log\epsilon},\frac{\log(1/2)}{\log\epsilon}]$, we have:

$$-\log\text{Precision@}K\leq\mathcal{L}_{\text{Talos}}+\log(1+e^2/2)^{1/\tau} \tag{A.4}$$

Theorem 3.1 is proven. Notably, we observe the trade-off in temperature setting: 1) a large τ contradicting with $\tau\leq\frac{\log(1/2)}{\log\epsilon}$ renders Eq.(A.3) not hold, leading Talos fails to serve as an upper bound; 2) τ is set too small would either contradict with Eq.(A.2) or increase the constant $\log(1+e^2/2)^{1/\tau}$, scaling the gap with Precision@K.

A.2 Proof of Theorem 3.2

Given $-\frac{1}{|\mathcal{P}_u|}\sum_{i\in\mathcal{P}_u}\log\sigma(s_{ui}-\beta_u^k)$ as constants do not affect optimization, the original DRO problem can be simplified as:

$$\max_{Q\in\mathbb{Q}}\mathbb{E}_{j\sim Q}\left[\log\sigma(s_{uj}-\beta_u^k)\right] \quad s.t. \quad \mathbb{Q}=\{Q:D_{\text{KL}}(Q\|\hat{Q})\leq\eta\} \tag{A.5}$$

Let $L=Q(j)/\hat{Q}(j)$ and define a convex function $\phi(x)=x\log x-x+1$, then the KL divergence can be written as $\mathbb{E}_{\hat{Q}}[\phi(L)]$. Let $g(u,j)=\log\sigma(s_{uj}-\beta_u^k)$, Eq.(A.5) can be reformulated as:

$$\max_{L}\mathbb{E}_{\hat{Q}}[g(u,j)L] \quad s.t. \quad \mathbb{E}_{\hat{Q}}[\phi(L)]\leq\eta \text{ and } \mathbb{E}_{\hat{Q}}[L]=1 \tag{A.6}$$

As a convex optimization problem, we use the Lagrangian function to solve it:

$$\min_{\tau\geq 0,\lambda}\max_{L}\left\{\mathbb{E}_{\hat{Q}}\left[g(u,j)L\right]-\tau\left(\mathbb{E}_{\hat{Q}}\left[\phi(L)\right]-\eta\right)+\lambda\left(\mathbb{E}_{\hat{Q}}[L]-1\right)\right\} \tag{A.7}$$

By the theorem of interchange of minimization and integration [39], we can interchange maximization and expectation in Eq.(A.7) as:

$$\text{Eq.(A.7)}\iff\min_{\tau\geq 0,\lambda}\left\{\tau\eta-\lambda+\tau\mathbb{E}_{\hat{Q}}\left[\max_{L}\left\{\frac{g(u,j)+\lambda}{\tau}L-\phi(L)\right\}\right]\right\} \tag{A.8}$$

Notice that $\max_{L}\left\{\frac{g(u,j)+\lambda}{\tau}L-\phi(L)\right\}=\phi^*(\frac{g(u,j)+\lambda}{\tau})$ is the convex conjugate function of $\phi(x)$, and we have $\phi^*(x)=e^x-1$. Then:

$$\text{Eq.(A.8)}=\min_{\tau\geq 0,\lambda}\left\{\tau\eta-\lambda+\tau\mathbb{E}_{\hat{Q}}\left[\exp(\frac{g(u,j)+\lambda}{\tau})-1\right]\right\} \tag{A.9}$$

The optimal λ^*, which minimizes the preceding expression is $\lambda^* = -\tau \log \mathbb{E}_{\hat{Q}}\left[\exp(g(u,j)/\tau)\right]$. Ultimately, substituting λ^*, $g(u,j) = \log \sigma(s_{uj} - \beta_u^k)$ back into Eq.(A.9), we have:

$$
\begin{aligned}
\text{Eq.(A.9)} &= \min_{\tau \geq 0}\left\{\tau\eta + \tau \log \mathbb{E}_{\hat{Q}}\left[\exp(\frac{g(u,j)}{\tau})\right]\right\} \\
&= \min_{\tau \geq 0}\left\{\tau\eta + \tau \log \mathbb{E}_{\hat{Q}}\left[\sigma(s_{uj} - \beta_u^k)^{1/\tau}\right]\right\}
\end{aligned} \tag{A.10}
$$

Eq.(3.9) is equivalent to optimizing:

$$
\begin{aligned}
&-\frac{1}{|\mathcal{P}_u|}\sum_{i\in\mathcal{P}_u}\log\sigma(s_{ui}-\beta_u^k) + \tau\log\mathbb{E}_{\hat{Q}}\left[\sigma(s_{uj}-\beta_u^k)^{1/\tau}\right] \\
&= \tau\cdot\underbrace{\left(-\frac{1}{|\mathcal{P}_u|}\sum_{i\in\mathcal{P}_u}\frac{1}{\tau}\log\sigma(s_{ui}-\beta_u^k) + \log\mathbb{E}_{\hat{Q}}\left[\sigma(s_{uj}-\beta_u^k)^{1/\tau}\right]\right)}_{\text{Talos}}
\end{aligned}
$$

A.3 Proof of Theorem 3.3

We begin by calculating the accurate gradient w.r.t. $\mathbf{s}_u$ (the vector of all predicted scores) as follows:

$$
\nabla_{\mathbf{s}_u}\mathcal{L}_{\text{Talos}}(\mathbf{s}_u, \beta_u^K(\mathbf{s}_u)) = \frac{\partial\mathcal{L}_{\text{Talos}}}{\partial\mathbf{s}_u} + \frac{\partial\mathcal{L}_{\text{Talos}}}{\partial\beta_u^K}\frac{\partial\beta_u^K}{\partial\mathbf{s}_u}
$$

For simplicity, let $g = \frac{\partial\mathcal{L}_{\text{Talos}}}{\partial\mathbf{s}_u}$ and $q = \frac{\partial\mathcal{L}_{\text{Talos}}}{\partial\beta_u^K}\frac{\partial\beta_u^K}{\partial\mathbf{s}_u}$. In practical implementation, we detach the term q. In fact, this omission does not affect convergence. We prove this with the following four steps:

Step 1: Approximation of Quantile Regression Loss. Since it has been proved in Appendix H.1 that Eq.(3.3) is unbiased, we analyze the original Eq.(H.8) for simplicity. For theoretical rigor, the following form is used, which is equivalent to Eq.(H.8):

$$
\mathcal{L}_{\text{QR-2}}(\beta;\mathbf{s}_u) := \frac{K+\epsilon}{|\mathcal{I}|}\beta + \frac{1}{|\mathcal{I}|}\sum_{i\in\mathcal{I}}(s_{ui}-\beta)_+ \tag{A.11}
$$

where ϵ is a sufficiently small constant to ensure the uniqueness of the solution. To bound q, we need derive the term $\frac{\partial\beta_u^K}{\partial\mathbf{s}_u}$. However, the non-smooth term $(\cdot)_+$ in Eq.(A.11) hinders the derivation. Since $(\cdot)_+$ can be approximated by the softplus function $\phi(x) = \kappa\ln(1+\exp(\cdot/\kappa))$ as $\kappa\to 0$, we approximate Eq.(A.11) with:

$$
\mathcal{L}_{\text{QR-S}}(\beta;\mathbf{s}_u):=\frac{K+\epsilon}{|\mathcal{I}|}\beta + \frac{\mu}{2}\beta^2 + \frac{1}{|\mathcal{I}|}\sum_{i\in\mathcal{I}}\kappa\ln\left(1+\exp((s_{ui}-\beta)/\kappa)\right) \tag{A.12}
$$

where $\frac{\mu}{2}\beta^2$ ensures its μ-strongly convex. We prove that the difference between $\beta_{u\text{-}S}^k$ (optimal solution of Eq.(A.12)) and β_u^k (optimal solution of Eq.(A.11)) is negligible, which justifies the use of $\mathcal{L}_{\text{QR-S}}$.

Proof. Since $x_+ \leq \phi(x) \leq x_+ + \kappa\ln 2$, we have:

$$
\mathcal{L}_{\text{QR-2}}(\beta;\mathbf{s}_u) \leq \mathcal{L}_{\text{QR-S}}(\beta;\mathbf{s}_u) \leq \mathcal{L}_{\text{QR-2}}(\beta;\mathbf{s}_u) + \frac{\mu}{2}\beta^2 + \epsilon^2\ln 2 \tag{A.13}
$$

Let $A = \frac{\mu}{2}(\beta_u^k)^2 + \epsilon^2\ln 2$, we have:

$$
-\mathcal{L}_{\text{QR-2}}(\beta_u^k;\mathbf{s}_u) \leq -\mathcal{L}_{\text{QR-S}}(\beta_u^k;\mathbf{s}_u)+A \leq -\mathcal{L}_{\text{QR-S}}(\beta_{u\text{-}S}^K;\mathbf{s}_u)+A \tag{A.14}
$$

Thus, we have:

$$
\mathcal{L}_{\text{QR-2}}(\beta_{u\text{-}S}^K;\mathbf{s}_u)-\mathcal{L}_{\text{QR-2}}(\beta_u^k;\mathbf{s}_u) \leq \mathcal{L}_{\text{QR-2}}(\beta_{u\text{-}S}^K;\mathbf{s}_u)-\mathcal{L}_{\text{QR-S}}(\beta_{u\text{-}S}^K;\mathbf{s}_u)+A \tag{A.15}
$$

Since $\mathcal{L}_{\text{QR-2}}(\beta_{u\text{-}S}^K;\mathbf{s}_u)-\mathcal{L}_{\text{QR-S}}(\beta_{u\text{-}S}^K;\mathbf{s}_u)\leq 0$ and $\beta_u^k\in[-1,1]$, we have:

$$
\mathcal{L}_{\text{QR-2}}(\beta_{u\text{-}S}^K;\mathbf{s}_u) - \mathcal{L}_{\text{QR-2}}(\beta_u^k;\mathbf{s}_u)\leq A \leq \frac{\epsilon^2}{2} + \epsilon^2\ln 2 = O(\epsilon^2) \tag{A.16}
$$

Considering the sub-gradient of $\mathcal{L}_{\text{QR-2}}$ w.r.t. β_u^k, i.e., $\partial\mathcal{L}_{\text{QR-2}}(\beta_u^k;\mathbf{s}_u) = \left[\frac{\epsilon-1}{|\mathcal{I}|}, \frac{\epsilon}{|\mathcal{I}|}\right]$, we can analyze the two cases:

- Condition: $\beta_{u\text{-}S}^K \geq \beta_u^k$, take the sub-gradient $g_1 = \epsilon/|\mathcal{I}| \geq 0$:

$$
|\beta_{u\text{-}S}^K - \beta_u^k| \leq \frac{1}{|g_1|}\left(\mathcal{L}_{\text{QR-2}}(\beta_{u\text{-}S}^K;\mathbf{s}_u)-\mathcal{L}_{\text{QR-S}}(\beta_u^k;\mathbf{s}_u)\right) = O(\epsilon) \tag{A.17}
$$

- $\beta_{u\text{-}S}^K < \beta_u^k$, take the sub-gradient $g_1 = (\epsilon - 1)/|\mathcal{I}| \geq 0$:

$$
|\beta_{u\text{-}S}^K - \beta_u^k| \leq \frac{1}{|g_2|}\left(\mathcal{L}_{\text{QR-2}}(\beta_{u\text{-}S}^K;\mathbf{s}_u)-\mathcal{L}_{\text{QR-S}}(\beta_u^k;\mathbf{s}_u)\right) = O(\epsilon^2) \leq O(\epsilon) \tag{A.18}
$$

In all the cases, we have $|\beta_{u\text{-}S}^K - \beta_u^k| \leq O(\epsilon)$, indicating that the surrogate $\mathcal{L}_{\text{QR-S}}$ does not affect the quantile estimation.

Step 2: The Gradient q bound. Suppose $|s_{ui} - \beta_u^k| \geq d$ for all i, we now bound the gradient norm $\|q\|$ as:

$$
\|q\| \leq \frac{2|\mathcal{I}|^{1/2}}{\tau}\frac{e^{-d/\kappa}}{\kappa^2} \quad \text{where} \quad q = \boxed{\frac{\partial\mathcal{L}_{\text{Talos}}}{\partial\beta_u^K}}\boxed{\frac{\partial\beta_u^K}{\partial\mathbf{s}_u}}
$$

(a) First term. The $\frac{\partial\mathcal{L}_{\text{Talos}}}{\partial\beta_u^k}$ term is bounded, as:

$$
\tau\frac{\partial\mathcal{L}_{\text{Talos}}}{\partial\beta_u^k} = \sum_{i\in\mathcal{P}_u}\frac{\sigma(\beta_u^k - s_{ui})}{|\mathcal{P}_u|} - \sum_{j\in\mathcal{N}_u}\frac{\sigma_\tau(s_{uj}-\beta_u^k)}{\sum_{v\in\mathcal{N}_u}\sigma_\tau(s_{uv}-\beta_u^k)}\sigma(\beta_u^k - s_{uj}) \tag{A.19}
$$

Since sigmoid function satisfies $0 \leq \sigma(x) \leq 1$, $\|\frac{\partial\mathcal{L}_{\text{Talos}}}{\partial\beta_u^k}\| \leq 2/\tau$.

(b) Second term. Given by the first-order optimality condition, we have $\frac{\partial\mathcal{L}_{\text{QR-S}}}{\partial\beta_u^k} = 0$. Take the gradient w.r.t. $\mathbf{s}_u$, we have:

$$
0=\frac{\partial^2\mathcal{L}_{\text{QR-S}}}{\partial(\beta_u^k)^2}\frac{\partial\beta_u^k}{\partial\mathbf{s}_u} + \frac{\partial^2\mathcal{L}_{\text{QR-S}}}{\partial\beta_u^k\partial\mathbf{s}_u} \to \nabla_{\mathbf{s}_u}\beta_u^k=-\left[\nabla_{\beta_u^k}^2\mathcal{L}_{\text{QR-S}}\right]^{-1}\nabla_{\beta_u^k,\mathbf{s}_u}^2\mathcal{L}_{\text{QR-S}} \tag{A.20}
$$

Given $\sigma(x)\sigma(-x) \geq 0$, and set μ as κ, we have:

$$
\nabla_{\beta_u^k}^2\mathcal{L}_{\text{QR-S}} = \mu + \frac{1}{\kappa|\mathcal{I}|}\sum_{i\in\mathcal{I}}\sigma\left((s_{ui}-\beta_u^k)/\kappa\right)\sigma\left((\beta_u^k-s_{ui})/\kappa\right) \geq \kappa \tag{A.21}
$$

We derive second-order gradient as:

$$
\nabla_{\beta_u^k,\mathbf{s}_u}^2\mathcal{L}_{\text{QR-S}} = \frac{1}{\kappa|\mathcal{I}|}\left[\sigma\left((s_{ui}-\beta_u^k)/\kappa\right)\sigma\left((\beta_u^k-s_{ui})/\kappa\right)\right]_{i=1}^{|\mathcal{I}|} \tag{A.22}
$$

$\sigma(x)\sigma(-x)$ is an even function that satisfies $\sigma(x)\sigma(-x)=\sigma(|x|)\sigma(-|x|) \leq \exp(|x|)$. Given $|s_{ui} - \beta_u^k| \geq d$, we have $\nabla_{\beta_u^k,\mathbf{s}_u}^2\mathcal{L}_{\text{QR-S}} \leq e^{-d/\kappa}/\kappa\cdot\mathbf{1}$, where $\mathbf{1}$ is a vector of ones with length $|\mathcal{I}|$. Therefore, we have $\|\nabla_{\mathbf{s}_u}\beta_u^k\| \leq |\mathcal{I}|^{1/2}\cdot e^{-d/\kappa}/\kappa^2$.

Given the First term and Second term bound, we conclude:

$$
\|q\| \leq \frac{2|\mathcal{I}|^{1/2}}{\tau}\frac{e^{-d/\kappa}}{\kappa^2} \implies \|q\| \to 0 \text{ as } \kappa \to 0 \tag{A.23}
$$

Step 3: Convergence Guarantee. Let K be the Lipschitz constant of $\mathcal{L}_{Talos}$, and $\theta_1^{(t)}$ denotes parameters that are updated at iteration

Table A.1: Temporal shift exploration.

Loss	Gowalla		Games	
	Precision@20	Recall@20	Precision@20	Recall@20
SL@K	0.0567	0.1559	0.0091	0.0708
Talos	**0.0574**	**0.1577**	**0.0094**	**0.0738**
Imp.%	**+1.12%**	**+1.12%**	**+2.95%**	**+4.15%**

Table A.3: Performance comparison with varying K on Movie-Lens. P@K denotes Precision@K.

Loss	P@20	P@50	P@80	P@100	P@200	P@400
SL@K	0.2287	0.1557	0.1224	0.1067	0.0685	0.0400
Talos	**0.2349**	**0.1600**	**0.1257**	**0.1101**	**0.0700**	**0.0410**
Imp.%	**+2.70%**	**+2.76%**	**+2.65%**	**+3.21%**	**+2.16%**	**+2.26%**

t with q detached. For convenience, we simplify notation $g(\theta_1^{(t)})$ as $g^{(t)}$, $q(\theta_1^{(t)})$ as $q^{(t)}$, and $\mathcal{L}_{\text{Talos}}(\theta_1^{(t)})$ as $\mathcal{L}_{\text{Talos}}^{(t)}$. We can derive:

$$
\begin{aligned}
\mathcal{L}_{\text{Talos}}^{(t+1)} &\leq \mathcal{L}_{\text{Talos}}^{(t)} - \left\langle g^{(t)} + q^{(t)}, \alpha g^{(t)} \right\rangle + \frac{K}{2}\alpha^2 \|g^{(t)}\|^2 \\
&= \mathcal{L}_{\text{Talos}}^{(t)} - \alpha\left\langle g^{(t)}, q^{(t)} \right\rangle - (\alpha - \frac{K}{2}\alpha^2)\|g^{(t)}\|^2 \qquad \text{(A.24)} \\
&\leq \mathcal{L}_{\text{Talos}}^{(t)} + \alpha\|g^{(t)}\|\|q^{(t)}\| - (\alpha - \frac{K}{2}\alpha^2)\|g^{(t)}\|^2
\end{aligned}
$$

Let $c = \alpha - \frac{K}{2}\alpha^2$, take $0 < \alpha < \frac{2}{K}$, we have $c\sum_{t=0}^{T}\|g^{(t)}\|^2 \leq \mathcal{L}_{\text{Talos}}^{(0)} + \alpha\sum_{t=0}^{T}\|q^{(t)}\|\|g^{(t)}\|$. With Young inequality, we have: $\alpha\|q^{(t)}\|\|g^{(t)}\| \leq \frac{c}{2}\|g^{(t)}\|^2 + \frac{\alpha^2}{2c}\|q^{(t)}\|^2$. Therefore, we obtain:

$$
\frac{c}{2}\|g^{(t)}\|^2 \leq \mathcal{L}_{\text{Talos}}^{(0)} + \frac{\alpha^2}{2c}\sum_{t=0}^{T}\|q^{(t)}\|^2 \qquad \text{(A.25)}
$$

We have proved in step 2 that $\|q\| \to 0$ as $\kappa \to 0$, thus we conclude:

$$
\frac{(2\alpha - K\alpha^2)}{4}\mathbb{E}_t\left[\|g^{(t)}\|^2\right] \leq \frac{1}{T}\mathcal{L}_{Talos}^{(0)} < \infty \implies \|g^{(T)}\|^2 \to 0 \qquad \text{(A.26)}
$$

Step 4: Convergence Equivalence. We additionally demonstrate that omitting q does not affect convergence to the same solutions: difference between $\theta_1^{(T)}$ (updated with q detach) and $\theta_2^{(T)}$ (updated by $g+q$) is negligible. Given two update schemes, we can derive:

$$
\theta_1^{(t+1)} = \theta_1^{(t)} - \alpha g(\theta_1^{(t)}) \quad \text{and} \quad \theta_2^{(t+1)} = \theta_2^{(t)} - \alpha\left(g(\theta_2^{(t)}) + q(\theta_2^{(t)})\right)
$$

For convenience, we simplify $\|\theta_2^{(t)} - \theta_1^{(t)}\|$ as B_t, and $q(\theta_2^{(t)})$ as $q^{(t)}$. Let L_g denotes the Lipschitz constant of $\nabla\mathcal{L}_{\text{Talos}}$, we have:

$$
\begin{aligned}
B_{t+1} &\leq B_t + \alpha\|g(\theta_2^{(t)}) - g(\theta_1^{(t)})\| + \alpha\|q^{(t)}\| \\
&\leq B_t + \alpha L_g B_t + \alpha\|q^{(t)}\| = (1 + \alpha L_g)B_t + \alpha\|q^{(t)}\|
\end{aligned} \qquad \text{(A.27)}
$$

Note that $B_0 = 0$. Given our conclusion in step 2, we have:

$$
B_t \leq \alpha\frac{2|\mathcal{I}|}{\tau}\frac{e^{-d/\kappa}}{\kappa^2}\sum_{k=0}^{t-1}(1 + \alpha L_g)^k = \frac{2|\mathcal{I}|}{\tau}\frac{e^{-d/\kappa}}{\kappa^2}\frac{(1 + \alpha L_g)^t - 1}{L_g}
$$

Let T denotes the maximum training step. $\forall\epsilon > 0$, take a small $\kappa \geq \sqrt{2|\mathcal{I}|\left((1 + \alpha L_g)^T - 1\right)/\tau\epsilon L_g}$, we have $\|\theta_1^{(T)} - \theta_2^{(T)}\| \leq \epsilon$, indicating that two update schemes converge to the same optimal solutions.

Table A.2: Number of negative samples exploration.

Loss	Beauty			MovieLens		
	$|G_u| = 8$	$|G_u| = 16$	$|G_u| = 32$	$|G_u| = 8$	$|G_u| = 16$	$|G_u| = 32$
SL@K	0.0167	0.0159	0.0150	0.2242	0.2265	0.2215
Talos	**0.0173**	**0.0162**	**0.0156**	**0.2310**	**0.2311**	**0.2266**
Imp.%	**+3.67%**	**+1.96%**	**+3.50%**	**+3.01%**	**+2.02%**	**+2.28%**

Table A.4: The error between the estimated Top-K quantile $\hat{\beta}_u^{20}$ and the ideal Top-K quantile β_u^{20}.

Loss	Gowalla	Beauty	Games	MovieLens
SL@K	0.1943	0.1948	0.2028	0.1389
Talos	0.0131	0.0123	0.0100	0.0059

B SL@K Comparison

We present a comparative study between SL@K [58] and Talos across multiple evaluation scenarios. We also refer to Yang et al. [58], and conduct additional comparisons on MovieLens dataset to extend the evaluation scope.

We first argue that NDCG@K also exhibits significant difference from Top-K accuracy. As shown in Table 1.1, optimizing NDCG@K may not always yield better Top-K accuracy. This observation indicates that SL@K, while tailored to NDCG@K, may fail to deliver proportional improvements in Top-K accuracy. Table A.3 also demonstrates this: With varying K, Talos consistently outperforms SL@K +2.62% on average in terms of Top-K accuracy metric, underscoring the importance of directly optimizing Top-K accuracy in practical recommendation scenarios.

Table A.2 shows that Talos achieves an average improvement of +2.83%, whereas SL@K shows reduced robustness under limited negative numbers. In temporal shift scenario, Talos achieves an average improvement of +2.84% over SL@K. This superiority reflects the inherent connection between Talos and DRO (*cf.* Theorem 3.2). While prior work [52] demonstrates the connection between SL and *Distributionally Robustness Optimization*, we attribute the performance drop to the additional weight term introduced in SL@K. In addition, Talos incorporates a more accurate threshold estimation strategy, resulting in substantially lower estimation error than SL@K (*cf.* Table A.4).

C Detailed Related Work

In this section, we presnet the detailed related work on **recommendation models** and **recommendation loss consistency**.
Recommendation Models. In the realm of RS, recommendation models play a vital role in anticipating the user preference. Among various architectures, collaborative filtering (CF) [9, 45, 68] is widely adopted to instruct the model design. The primary task of CF-models is to predict interactions by assessing the similarity between user and item embeddings. Early research focused on Matrix Factorization (MF) [26], which decomposes the user-item interaction matrix into latent user and item embedding vectors. This approach act as foundational models like MF [26], SVD [1] and NCF [17]. The more advanced methods, inspired by the efficacy of Graph Neural Networks (GNNs [6, 7, 51, 55]), including LightGCN [16], NGCF [51], LCF [60], and APDA [66], have emerged and achieve great success to address this issue. Recently, some works attempt to introduce contrastive learning paradigm into LightGCN to augment

graph data such as XSimGCL [59], etc, achieving the state-of-the-art performance. In addition, several recent works utilized large language models [11, 48, 49] to enhance RS performance.

Recommendation Loss Consistency. Recent studies [30, 36, 56] have theoretically demonstrated the loss consistency in terms of recommendation metrics. In particular, Long and Servedio [30], Wydmuch et al. [56] have demonstrated H-consistency and Bayes-consistency for SL w.r.t. Precision@*K*, respectively. Pu et al. [36] further demonstrate the consistency of SL in two-tower recommendation model settings. However, practical recommendation tasks are inherently complex: distribution shifts, sparse interactions, and limited model capacity mean that the Bayes and H-consistency optimal situation is rarely attainable in practice. Consequently, substantial performance disparities among SL-based methods were observed in empirical experiments (*cf.* Tables 3.1 and 3.4). This necessitates examining their consistency in practical RS scenarios.

D Experimental Details

D.1 Inconsistency Simulation Details

To quantify the inconsistency between LLPAUC/NDCG and Top-*K* metrics (*i.e.*, Recall@*K* and NDCG@*K*), we simulate pair-wise comparisons of ranking lists as follows: We randomly generate two ranking lists, in which the elements represent the ranking of positive items ($\pi_{ui} \leq 200$ for simulating the real-world recommender systems). Afterwards, we compute NDCG, LLPAUC, and Top-*K* metrics (*i.e.*, Precision@20, NDCG@20) for both lists. An inconsistency case occurs when one list achieves higher NDCG/LLPAUC but lower Top-K accuracy compared to the other, *i.e.*, optimizing LLPAUC/NDCG does not bring benefits for improving Top-*K* metrics. The ratio of such cases is collected over 10,000 independent trials (per dataset) to ensure statistical stability.

D.2 Recommendation Backbones

In our experiments, we implement three popular recommendation backbones:
- **MF** [26]: MF is the most foundational yet effective model that factorizes user-item interactions into learnable embeddings (user embedding and item embedding). All the embedding-based recommendation models use MF as the first layer. Following Wang et al. [51], we implement MF with embedding dimension $d = 64$ for all settings.
- **LightGCN** [16]: LightGCN is a effective GNN-based recommendation model that aggregates high-order user-item interactions via non-parameterized graph convolution. By eliminating non-linear activations and feature transformations in NGCF [51], LightGCN achieves computational efficiency and enhanced performance. In our experiments, we adopt 2 graph convolution layers, which aligns with the original setting in He et al. [16].
- **XSimGCL** [59]: XSimGCL is a novel contrastive learning enhanced [20, 29] variant of 3-layer LightGCN that injects random noise into intermediate embeddings, and optimizes an auxiliary InfoNCE loss [32] between the final layer and a selected intermediate layer (l^*). Following the original Yu et al. [59]'s setting, the modulus of random noise between each layer is set as 0.1, the contrastive layer l^* is set as 1 (where the embedding layer is 0-th

Table D.1: Dataset statistics.

Dataset	#Users	#Items	#Interactions	Density
Electronics	150,523	52,024	1,312,545	0.0007
Gowalla	29,858	40,988	1,027,464	0.0007
Games	18,813	8,691	177,572	0.0009
Beauty	15,603	8,693	139,554	0.0009

layer), the temperature of InfoNCE is set as 0.1, and the weight of the auxiliary InfoNCE loss is searching from {0.01, 0.05, 0.1, 0.2}.

D.3 Datasets

The four benchmark datasets used in our experiments are summarized in Table D.1. Following [15, 51], we use 10-core setting (or 5-core setting) for Gowalla (or Amazon) dataset. Following Yang et al. [57], we further clean the data by excluding interactions with ratings below 3 (if available). The dataset is randomly split into training set, validation set, and test set in a ratio of 7:1:2. The details of datasets are as follows:
- **Gowalla** [16]: A check-in dataset from the location-based social network Gowalla[2], which consists of 1M users, 1M locations, and 6M check-ins.
- **Movielens** [14]: The Movielens dataset is a movie rating dataset collected from Movielens[3]. We use the Movielens-100K version, which contains 100,000 ratings from 1000 users on 1700 movies.
- **Amazon:** Subsets of the 2014 Amazon product review corpus[4], which contains 142.8 million reviews spanning May 1996 to July 2014. We process three widely-used categories: Beauty, Games and Electronics [57], with interactions ranging from 40K to 1M.

D.4 Recommendation Scenarios

The detailed dataset constructions in IID and distributional shift settings are as follows:
- **IID setting.** Following the standard recommendation setup [16], we i.i.d. split training and test sets from the complete dataset, maintaining identical distributions between both sets. Specifically, the positive items of each user are split into 80% training and 20% test sets. Moreover, the training set is further split into 90% training and 10% validation sets for hyperparameter tuning.
- **Distributional shift setting.** We follow [47], introducing temporal bias to construct the test scenario with distribution shifts — we divide the training and test dataset according to the interaction time. Specifically, interactions with timestamps in the earliest 80% constitute the training set, while the latest 20% form the test set. Additionally, we randomly split 10% of the training set as the validation set. The temporal shift is very common in real recommendation systems, as user preferences typically evolve over time [50].

D.5 Hyperparameter Setting

Following [53], the latent embedding size is set as 64. For model training, we adopt Adam [23] optimizer with the learning rate

---

[2]https://en.wikipedia.org/wiki/Gowalla
[3]https://movielens.org/
[4]https://cseweb.ucsd.edu/~jmcauley/datasets/amazon/links.html

Shengjia Zhang, Weiqin Yang, Jiawei Chen, Peng Wu, Yuegang Sun, Gang Wang, Qihao Shi, and Can Wang

Table D.2: Overall performance comparison of Talos with other losses. `blue` **indicates the Talos achieves the SOTA performance, and the runner-up is underlined. Imp.% indicates the relatively improvements of Talos over the best baselines. The mark '*' suggests the improvement is statistically significant with $p < 0.05$.**

Model	Loss	Gowalla		Beauty		Games		Electronics	
		MRR@20	NDCG@20	MRR@20	NDCG@20	MRR@20	NDCG@20	MRR@20	NDCG@20
MF	BPR	0.0340	0.1167	0.0374	0.0698	0.0339	0.0699	0.0155	0.0303
	AATP	0.0227	0.0795	0.0294	0.0558	0.0318	0.0674	0.0065	0.0135
	RS@K	0.0301	0.0972	0.0223	0.0374	0.0232	0.0458	0.0050	0.0088
	SmoothI@K	0.0449	0.1473	0.0443	0.0778	0.0492	0.0973	0.0180	0.0329
	SL	0.0481	0.1585	0.0470	0.0813	0.0511	0.1027	0.0175	0.0339
	BSL	0.0481	0.1585	<u>0.0470</u>	0.0813	<u>0.0514</u>	0.1035	0.0177	0.0341
	PSL	<u>0.0485</u>	<u>0.1595</u>	0.0469	<u>0.0820</u>	0.0514	<u>0.1035</u>	<u>0.0183</u>	<u>0.0350</u>
	AdvInfoNCE	0.0481	0.1582	0.0468	0.0811	0.0505	0.1027	0.0180	0.0341
	LLPAUC	0.0444	0.1459	0.0395	0.0737	0.0450	0.0922	0.0134	0.0285
	Talos	**0.0513**	**0.1667**	**0.0482**	**0.0851**	**0.0532**	**0.1063**	**0.0190**	**0.0361**
	Imp.%	**+5.84%***	**+4.49%***	**+2.39%***	**+3.77%***	**+3.35%***	**+2.69%***	**+3.63%***	**+3.15%***
LGCN	BPR	0.0425	0.1398	0.0412	0.0762	0.0467	0.0952	0.0128	0.0251
	AATP	0.0153	0.0533	0.0290	0.0560	0.0262	0.0574	0.0069	0.0144
	RS@K	0.0392	0.1321	0.0410	0.0695	0.0414	0.0816	0.0103	0.0195
	SmoothI@K	0.0444	0.1472	0.0456	0.0811	0.0496	0.0981	0.0196	<u>0.0362</u>
	SL	0.0480	0.1584	0.0458	0.0810	<u>0.0514</u>	<u>0.1035</u>	0.0176	0.0340
	BSL	0.0480	0.1584	0.0458	0.0810	0.0511	0.1031	0.0175	0.0338
	PSL	<u>0.0490</u>	<u>0.1608</u>	<u>0.0462</u>	<u>0.0813</u>	0.0514	0.1031	0.0179	0.0343
	AdvInfoNCE	0.0481	0.1587	0.0458	0.0811	0.0513	0.1032	0.0175	0.0338
	LLPAUC	0.0415	0.1367	0.0447	0.0803	0.0505	0.1012	0.0179	0.0346
	Talos	**0.0517**	**0.1675**	**0.0478**	**0.0848**	**0.0528**	**0.1056**	0.0190	**0.0363**
	Imp.%	**+5.66%***	**+4.17%***	**+3.55%***	**+4.20%***	**+2.71%***	**+2.00%***	−	**+0.13%***
XSimGCL	BPR	0.0469	0.1531	0.0447	0.0812	0.0483	0.0976	0.0177	0.0339
	AATP	0.0311	0.1108	0.0396	0.0707	0.0398	0.0833	0.0134	0.0264
	RS@K	0.0364	0.1251	0.0401	0.0697	0.0402	0.0824	0.0100	0.0195
	SmoothI@K	0.0379	0.1299	0.0181	0.0312	0.0330	0.0684	0.0118	0.0224
	SL	0.0475	0.1568	0.0457	0.0805	0.0503	0.1017	0.0175	0.0338
	BSL	0.0475	0.1572	0.0438	0.0788	0.0504	0.1023	0.0168	0.0330
	PSL	0.0480	<u>0.1583</u>	<u>0.0463</u>	0.0808	0.0505	0.1019	<u>0.0181</u>	<u>0.0348</u>
	AdvInfoNCE	0.0475	0.1568	0.0456	0.0803	0.0502	0.1019	0.0175	0.0337
	LLPAUC	<u>0.0481</u>	0.1571	0.0459	<u>0.0820</u>	<u>0.0517</u>	<u>0.1037</u>	0.0181	0.0347
	Talos	**0.0506**	**0.1645**	**0.0489**	**0.0858**	**0.0526**	**0.1057**	**0.0189**	**0.0359**
	Imp.%	**+5.18%***	**+3.88%***	**+5.47%***	**+4.60%***	**+1.84%***	**+1.97%***	**+4.15%***	**+3.25%***

in the range $\{10^{-1}, 10^{-2}, 10^{-3}\}$, except for BPR which uses an extended search lr $\in \{10^{-1}, 10^{-2}, 10^{-3}, 10^{-4}\}$. The weight decay (**wd**) is searched in $\{0, 10^{-4}, 10^{-6}, 10^{-8}\}$, except for BPR which uses an extended search wd $\in \{0, 10^{-3}, 10^{-4}, 10^{-5}, 10^{-6}, 10^{-8}\}$. The learning rate of the quantile estimation in Talos is fixed as 10^{-3}. Compared with SL, Talos preserves simplicity in hyperparameter tuning, requiring only a single temperature parameter τ. On XSimGCL backbone, we follow [59] tune the weight of the auxiliary InfoNCE (**wl**) in $\{0.2, 0.1, 0.05, 0.01\}$. Following He et al. [16], we adopt early stopping strategy, in which the training stops if Precision@20 metric fails to improve for 25 consecutive epochs in validation set. Following [53], we uniformly sample 1024 negative items for each positive instance in training (BPR only samples one).

Hyperparameter Settings. To maintain the fairness across all methods, we tune each methods with a very fine granularity to ensure their optimal performance. We reproduced the following losses as baselines in our experiments:

- **BPR:** No other hyperparameters.
- **AATP:** The quantile regression learning rate: $\text{lr}_{\text{quantile}} \in \{10^{-1}, 10^{-2}, 10^{-3}, 10^{-4}\}$.
- **RS@K:** The temperature τ_1, which approximates postive ranking, is searched in the range $\{0.01, 0.05, 0.10, 0.15, 0.20, 0.25, 0.30\}$. The temperature τ_2, which approximates the Heaviside function, is searched in $\{1, 2, 3, 4, 5\}$.
- **SL:** The temperature $\tau \in \{0.05, 0.10, 0.15, 0.2, 0.25, 0.30\}$.
- **SmoothI@K:** The temperature τ is searched in the same space as SL. Following the original setting Thonet et al. [46] offset δ is searched in the rang $\{0.05, 0.1, 0.15, 0.2, 0.25, 0.30\}$.
- **BSL:** The temperatures τ_1, τ_2 for positive and negative terms are searched in the same space as SL, respectively.

- **PSL:** The temperature τ is searched in the same space as SL. Following Yang et al. [57], the activation function is used as $\sigma(\cdot) = \tanh(\cdot/2)$ for its uniformly SOTA performance.
- **AdvInfoNCE:** The temperature τ is searched in the same space as SL. Following the original setting Zhang et al. [61], the other hyperparameters including: the negative weight is set as 64, the adversarial learning interval T_{adv} is searched in $\{5, 10, 15, 20\}$, the total adversarial training times E_{adv} is searched in $\{5, 10, 15, 20, 25, 30\}$, the adversarial learning rate is searched in $\{10^{-4}, 10^{-5}\}$.
- **LLPAUC:** hyperparameters $\alpha \in \{0.1, 0.3, 0.5, 0.7, 0.9\}$ and $\beta \in \{0.01, 0.1\}$, which follows Shi et al. [43]'s setting.
- **Talos:** The temperatures τ are searched in the same space as SL. The learning rate of quantile regression is fixed as 10^{-3}. No additional hyperparameters.

For all compared methods, we closely follow configurations in their respective publications to ensure the optimal performance. All experiments are conducted on one NVIDIA GeForce RTX 4090.

E NDCG and MRR performance

NDCG and MRR performance in Table D.2. Since comparable trends were observed across different backbones, we only report MF results for brevity. While Talos targets optimizing Top-K accuracy, it also exhibits superiority on MRR@K and NDCG@K. The reason can be attributed to the close relations between these Top-K metrics, where NDCG@K and MRR@K is built on Precision@K.

F Training Efficiency

We evaluate the computational efficiency of Talos on matrix factorization (MF) models and compare it with baseline losses. Table F.1 provides the time complexity and practical computational time of Talos and baseline methods. As shown in Table F.1, Talos incurs comparable overhead to SL ($1.00-1.50\times$ runtime), aligning with our complexity analysis in Section 3.2.

Table F.1: Computational time (s / epoch) on MF. All methods adopt uniform negative sampling technique, with $|G_u| = 1024$.

Loss	Complexity	Games	Beauty	Gowalla	Electronics
BPR	$O(\bar{P}|\mathcal{U}||\hat{G}_u|)$	1.23	0.16	0.14	2.18
AATP	$O(\bar{P}|\mathcal{U}||\hat{G}_u|)$	5.38	0.54	0.68	7.84
RS@K	$O(\bar{P}|\mathcal{U}||\hat{G}_u|)$	4.58	0.43	0.37	7.30
SmoothI@K	$O(\bar{P}|\mathcal{U}||\hat{G}_u|K)$	7.13	0.93	0.63	10.54
SL	$O(\bar{P}|\mathcal{U}||\hat{G}_u|)$	4.79	0.42	0.31	7.01
BSL	$O(\bar{P}|\mathcal{U}||\hat{G}_u|)$	4.56	0.43	0.34	7.17
PSL	$O(\bar{P}|\mathcal{U}||\hat{G}_u|)$	4.96	0.42	0.35	7.15
AdvInfoNCE	$O(\bar{P}|\mathcal{U}||\hat{G}_u|)$	8.14	0.71	1.00	9.31
LLPAUC	$O(\bar{P}|\mathcal{U}||\hat{G}_u|)$	4.82	0.52	0.37	6.63
Talos	$O(2\bar{P}|\mathcal{U}||\hat{G}_u|)$	5.37	0.54	0.43	7.98

G Notations

We summarize the notations used in this paper as follows:

- Table G.1 provides notations that are used to drive the Talos loss function.
- Table G.2 provides notations that are used to demonstrate the connections between Talos and *Distributional Robustness Optimization.*

Table G.1: Notations for deriving Talos.

Notations	Descriptions
u	a user in the user set $\mathcal{U}$
i	an item in the item set $\mathcal{I}$
$\mathcal{P}_u$	the positive item set of user u
$\mathcal{N}_u$	the negative item set of user u
G_u	the sampled negative item set of user u
s_{ui}	the similarity score between item i and user u
π_{ui}	the ranking of item i in ranking list of user u
β_u^k	the Top-K quantile of user u
$\hat{\beta}_u$	the estimated Top-K quantile of user u
$Q_K(u)$	the unbiased quantile estimation loss
$\mathcal{L}_{\text{Talos}}$	the Talos loss
$\mathbb{I}(\cdot)$	the Indicator function
$\delta(\cdot)$	the Heaviside step function
σ	the sigmoid$(\cdot)$ activation function
σ_τ	the sigmoid$(\cdot)^{1/\tau}$ activation function

Table G.2: Notations for Theorem 3.2 and its Proof

Notations	Descriptions
$\mathbb{Q}$	the uncertainty set
$\hat{Q}$	the uniform distribution of negative item set $\mathcal{N}_u$
Q	the pertubed distribution of $\hat{Q}$

Table G.3: Notations for Theorem 3.3 and its Proof

Notations	Descriptions
$\mathbf{s}_u$	the vector of all predicted scores of user u
$\nabla_{\mathbf{s}_u}$	the Talosgradient w.r.t. $\mathbf{s}_u$
$\nabla_{\beta_u^k}$	the Talosgradient w.r.t. β_u^k
g	the abbreviation for $\frac{\partial \mathcal{L}_{\text{Talos}}}{\partial \mathbf{s}_u}$ term
q	the abbreviation for $\frac{\partial \mathcal{L}_{\text{Talos}}}{\partial \beta_u^K} \frac{\partial \beta_u^K}{\partial \mathbf{s}_u}$ term
ϵ	the sufficiently small constant
κ	the hyperparameter in softplus function
$\mathcal{L}_{\text{QR-2}}$	the equivalent form of quantile regression loss
$\mathcal{L}_{\text{QR-S}}$	the convex appxmiation form of $\mathcal{L}_{\text{QR-2}}$
$\beta_{u\text{-S}}^K$	the optimal solution of $\mathcal{L}_{\text{QR-S}}$
T	the total optimization step
θ_1^T	the model parameter updated with g
θ_2^T	the model parameter updated with $g + q$
α	the fixed step-size in gradient decent
L_g	the Lipschiz constant of $\nabla \mathcal{L}_{\text{Talos}}$

Table G.4: Notations for Quantile Regression

Notations	Descriptions
$U(\mathcal{I})$	the uniform distribution of item set $\mathcal{I}$
S	the random variable of the score of items s_{ui}
F_S	the cumulative distribution function w.r.t. S

- Table G.3 provides notations that are used to demonstrate the convergence property of Talos and its corresponding proof.
- Table G.4 provides notations that are used to demonstrate the vanilla quantile regression and the proof in terms of our unbiased quantile regression loss.

H Quantile Regression

Quantile regression method [13, 25] is uniformly used for sample quantile estimation. The Top-K quantile is estimated by the following loss:

$$\mathcal{L}_{\text{QR}}(u) = \frac{1}{|\mathcal{I}|} \sum_{i \in \mathcal{I}} \left((1 - \frac{K}{|\mathcal{I}|})(s_{ui} - \hat{\beta}_u)_+ + \frac{K}{|\mathcal{I}|}(\hat{\beta}_u - s_{ui})_+ \right) \quad \text{(H.1)}$$

or equivalently:

$$\mathcal{L}_{\text{QR}}(u) = \mathbb{E}_{i \sim U(\mathcal{I})} \left[(1 - \frac{K}{|\mathcal{I}|})(s_{ui} - \hat{\beta}_u)_+ + \frac{K}{|\mathcal{I}|}(\hat{\beta}_u - s_{ui})_+ \right] \quad \text{(H.2)}$$

where $(\cdot)_+ = \max(\cdot, 0)$, and $U(\mathcal{I})$ denotes the uniform distribution on item set $\mathcal{I}$. The Top-K quantile is estimated as:

$$\beta_u^k = \underset{\hat{\beta}_u}{\arg\min} \, \mathcal{L}_{\text{QR}}(u) \quad \text{(H.3)}$$

We show this as follows:

Proof. Suppose that S is a random variable representing the score of items s_{ui}, and F_S is the c.d.f. of S on $\mathbb{R}$. Since $i \sim \mathcal{I}$ is uniformly distributed, the quantile regression loss (H.2) can be rewritten as the following expectation:

$$\mathcal{L}_{\text{QR}}(u) = \mathbb{E}_{S \sim F_S} \left[(1 - \frac{K}{|\mathcal{I}|})(S - \hat{\beta}_u)_+ + \frac{K}{|\mathcal{I}|}(\hat{\beta}_u - S)_+ \right]$$
$$= \int_{\hat{\beta}_u}^{\infty} (1 - \frac{K}{|\mathcal{I}|})(S - \hat{\beta}_u) \mathrm{d}F_S(S) + \int_{-\infty}^{\hat{\beta}_u} \frac{K}{|\mathcal{I}|}(\hat{\beta}_u - S) \mathrm{d}F_S(S) \quad \text{(H.4)}$$

Compute the derivative of $\mathcal{L}_{\text{QR}}(u)$ with respect to $\hat{\beta}_u$, set it to 0, and let $\beta_u = \arg\min_{\hat{\beta}_u} \mathcal{L}_{\text{QR}}(u)$, we have:

$$\frac{K}{|\mathcal{I}|} \int_{-\infty}^{\beta_u} \mathrm{d}F_S(S) = (1 - \frac{K}{|\mathcal{I}|}) \int_{\beta_u}^{\infty} \mathrm{d}F_S(S) \quad \text{(H.5)}$$

Given F_S is the c.d.f. of S on $\mathbb{R}$, we have:

$$F_S(\infty) = 1, \text{ and } F_S(-\infty) = 0 \quad \text{(H.6)}$$

Then, Eq.(H.5) can be derived as:

$$\frac{K}{|\mathcal{I}|} F_S(\beta_u) = \left(1 - \frac{K}{|\mathcal{I}|}\right)\left(1 - F_S(\beta_u)\right)$$
$$F_S(\beta_u) = \left(1 - \frac{K}{|\mathcal{I}|}\right) \quad \text{(H.7)}$$

resulting $\int_{\beta_u}^{\infty} \mathrm{d}F_S(S) = K/|\mathcal{I}|$, i.e., the optimal $\hat{\beta}_u$ is precisely the Top-K quantile of scores S. □

However, directly utilize Eq.(H.8) requires to traverse over the complete item space. In recommendation scenarios, the complete item space is huge, and computational intensive. To address this issue, we propose the efficient quantile estimation in Eq.(3.3), which supports sampling negative items to conduct unbiased Top-K quantile estimation. Table F.1 shows the training time cost in one epoch, indicating our proposed efficient quantile estimation is computational efficient.

H.1 Proof of Unbiased Eq.(3.3)

Quantile regression method [13, 25] is uniformly used for sample quantile estimation. Typically, the Top-K quantile is estimated by the following loss:

$$\mathcal{L}_{\text{QR}}(u) = \frac{1}{|\mathcal{I}|} \sum_{i \in \mathcal{I}} \left((1 - \frac{K}{|\mathcal{I}|})(s_{ui} - \hat{\beta}_u)_+ + \frac{K}{|\mathcal{I}|}(\hat{\beta}_u - s_{ui})_+ \right) \quad \text{(H.8)}$$

With expectation $\mathbb{E}_{G_u} \left[\sum_{j \in G_u} \rho_K(s_{uj} - \hat{\beta}_u) \right] = (|G_u|)/(|\mathcal{I}| - |\mathcal{P}_u|) \sum_{j \in \mathcal{N}_u} \rho_K(s_{uj} - \hat{\beta}_u)$, Eq.(3.3) can be derived as:

$$\mathbb{E}_{G_u}[Q_K(u)] = \frac{1}{|\mathcal{I}|} \left(\sum_{i \in \mathcal{P}_u} \rho_K(s_{ui} - \hat{\beta}_u) + \sum_{j \in \mathcal{N}_u} \rho_K(s_{uj} - \hat{\beta}_u) \right) = \mathcal{L}_{\text{QR}}(u)$$

I Optimal Hyperparameters

We report the optimal hyperparameters of each method on each dataset and backbone from Tables I.2 and I.3, in the order of the hyperparameters listed in Table I.1.

Table I.1: Hyperparameters to be searched for each method.

Method	Other Hyperparameters
BPR	no other hyperparameters
AATP	$\{\text{lr}_{\text{quantile}}\}$
RS@K	$\{\tau_{\text{inner}}, \tau_{\text{outside}}\}$
SmoothI@K	$\{\tau, \delta\}$
LLPAUC	$\{\alpha, \beta\}$
SL	$\{\tau\}$
AdvInfoNCE	$\{T_{\text{adv}}, E_{\text{adv}}, \text{lr}_{\text{adv}}, \tau\}$
BSL	$\{\tau_1, \tau_2\}$
PSL	$\{\tau\}$
Talos	$\{\tau\}$

Table I.2: Optimal hyperparameters of OOD setting.

Gowalla					
Model	Loss	lr	wd	wl	others
MF	BPR	10^{-3}	10^{-8}	N/A	
	AATP	10^{-3}	10^{-6}	N/A	$\{10^{-4}\}$
	RS@K	10^{-2}	10^{-8}	N/A	$\{0.05, 5\}$
	SmoothI@K	10^{-3}	0	N/A	$\{0.1, 0.1\}$
	SL	10^{-1}	0	N/A	$\{0.1\}$
	BSL	10^{-1}	0	N/A	$\{0.1, 0.1\}$
	PSL	10^{-1}	0	N/A	$\{0.05\}$
	AdvInfoNCE	10^{-1}	0	N/A	$\{5, 30, 10^{-5}, 0.1\}$
	LLPAUC	10^{-3}	10^{-6}	N/A	$\{0.7, 0.01\}$
	TL@K	10^{-1}	0	N/A	$\{0.05\}$
Games					
Model	Loss	lr	wd	wl	others
MF	BPR	10^{-3}	10^{-6}	N/A	
	AATP	10^{-3}	10^{-6}	N/A	$\{10^{-2}\}$
	RS@K	10^{-1}	10^{-8}	N/A	$\{0.05, 5\}$
	SmoothI@K	10^{-1}	0	N/A	$\{0.1, 0.05\}$
	SL	10^{-2}	0	N/A	$\{0.2\}$
	BSL	10^{-2}	0	N/A	$\{0.1, 0.2\}$
	PSL	10^{-2}	10^{-8}	N/A	$\{0.1\}$
	AdvInfoNCE	10^{-2}	0	N/A	$\{5, 5, 10^{-5}, 0.2\}$
	LLPAUC	10^{-3}	10^{-6}	N/A	$\{0.6, 0.7\}$
	TL@K	10^{-2}	10^{-6}	N/A	$\{0.1\}$

Table I.3: Optimal hyperparameters of IID setting.

Model	Loss	Gowalla				Beauty			
		lr	wd	wl	others	lr	wd	wl	others
MF	BPR	10^{-3}	10^{-8}	N/A		10^{-3}	10^{-6}	N/A	
	AATP	10^{-3}	10^{-6}	N/A	$\{10^{-4}\}$	10^{-2}	0	N/A	$\{10^{-3}\}$
	RS@K	10^{-1}	0	N/A	$\{0.01, 2\}$	10^{-1}	10^{-8}	N/A	$\{0.01, 1\}$
	SmoothI@K	10^{-3}	0	N/A	$\{0.1, 0.05\}$	10^{-1}	10^{-8}	N/A	$\{0.2, 0.05\}$
	SL	10^{-1}	0	N/A	$\{0.1\}$	10^{-3}	10^{-8}	N/A	$\{0.15\}$
	BSL	10^{-1}	0	N/A	$\{0.1, 0.1\}$	10^{-1}	0	N/A	$\{0.05, 0.15\}$
	PSL	10^{-1}	0	N/A	$\{0.05\}$	10^{-1}	0	N/A	$\{0.1\}$
	AdvInfoNCE	10^{-1}	0	N/A	$\{15, 25, 10^{-5}, 0.1\}$	10^{-1}	0	N/A	$\{15, 30, 10^{-5}, 0.15\}$
	LLPAUC	10^{-3}	10^{-6}	N/A	$\{0.8, 0.01\}$	10^{-2}	10^{-6}	N/A	$\{0.6, 0.9\}$
	Talos	10^{-2}	0	N/A	$\{0.05\}$	10^{-1}	10^{-8}	N/A	$\{0.1\}$
LGCN	BPR	10^{-3}	10^{-8}	N/A		10^{-3}	10^{-6}	N/A	
	AATP	10^{-3}	0	N/A	$\{10^{-2}\}$	10^{-3}	10^{-8}	N/A	$\{10^{-4}\}$
	RS@K	10^{-2}	0	N/A	$\{0.1, 5\}$	10^{-3}	0	N/A	$\{0.1, 5\}$
	SmoothI@K	10^{-3}	10^{-8}	N/A	$\{0.1, 0.05\}$	10^{-3}	10^{-8}	N/A	$\{0.2, 0.05\}$
	SL	10^{-1}	0	N/A	$\{0.1\}$	10^{-1}	0	N/A	$\{0.2\}$
	BSL	10^{-1}	0	N/A	$\{0.05, 0.1\}$	10^{-1}	0	N/A	$\{0.15, 0.2\}$
	PSL	10^{-2}	0	N/A	$\{0.05\}$	10^{-1}	0	N/A	$\{0.1\}$
	AdvInfoNCE	10^{-2}	0	N/A	$\{5, 30, 10^{-5}, 0.1\}$	10^{-1}	0	N/A	$\{5, 25, 10^{-5}, 0.2\}$
	LLPAUC	10^{-3}	10^{-8}	N/A	$\{0.1, 0.05\}$	10^{-2}	10^{-6}	N/A	$\{0.1, 0.1\}$
	Talos	10^{-2}	0	N/A	$\{0.05\}$	10^{-1}	0	N/A	$\{0.1\}$
XSimGCL	BPR	10^{-3}	0	0.05		10^{-2}	10^{-4}	0.2	
	AATP	10^{-4}	10^{-6}	0.05	$\{10^{-4}\}$	10^{-2}	10^{-8}	0.05	$\{10^{-3}\}$
	RS@K	10^{-2}	0	0.01	$\{0.1, 5\}$	10^{-3}	0	0.01	$\{0.15, 5\}$
	SmoothI@K	10^{-2}	0	0.01	$\{0.1, 0.1\}$	10^{-2}	0	0.01	$\{0.1, 0.05\}$
	SL	10^{-3}	0	0.01	$\{0.1\}$	10^{-3}	0	0.01	$\{0.2\}$
	BSL	10^{-2}	0	0.01	$\{0.05, 0.1\}$	10^{-3}	10^{-8}	0.01	$\{0.15, 0.02\}$
	PSL	10^{-1}	0	0.01	$\{0.05\}$	10^{-2}	0	0.01	$\{0.1\}$
	AdvInfoNCE	10^{-3}	0	0.01	$\{15, 30, 10^{-5}, 0.1\}$	10^{-3}	0	0.01	$\{10, 20, 10^{-5}, 0.2\}$
	LLPAUC	10^{-3}	10^{-8}	0.01	$\{0.1, 0.01\}$	10^{-2}	10^{-6}	0.01	$\{0.1, 0.01\}$
	Talos	10^{-1}	0	0.01	$\{0.05\}$	10^{-1}	0	0.01	$\{0.1\}$

Model	Loss	Games				Electronics			
		lr	wd	wl	others	lr	wd	wl	others
MF	BPR	10^{-2}	10^{-6}	N/A		10^{-3}	10^{-6}	N/A	
	AATP	10^{-3}	10^{-6}	N/A	$\{10^{-2}\}$	10^{-2}	0	N/A	$\{10^{-4}\}$
	RS@K	10^{-1}	10^{-8}	N/A	$\{0.05, 5\}$	10^{-3}	10^{-6}	N/A	$\{0.05, 5\}$
	SmoothI@K	10^{-2}	0	N/A	$\{0.15, 0.05\}$	10^{-3}	10^{-8}	N/A	$\{0.15, 0.2\}$
	SL	10^{-2}	10^{-6}	N/A	$\{0.2\}$	10^{-3}	10^{-6}	N/A	$\{0.2\}$
	BSL	10^{-1}	0	N/A	$\{0.05, 0.2\}$	10^{-2}	10^{-8}	N/A	$\{0.1, 0.2\}$
	PSL	10^{-1}	0	N/A	$\{0.1\}$	10^{-3}	10^{-8}	N/A	$\{0.1\}$
	AdvInfoNCE	10^{-1}	10^{-8}	N/A	$\{15, 5, 10^{-5}, 0.2\}$	10^{-2}	10^{-8}	N/A	$\{10, 30, 10^{-5}, 0.15\}$
	LLPAUC	10^{-2}	10^{-6}	N/A	$\{0.5, 0.9\}$	10^{-3}	10^{-6}	N/A	$\{0.6, 0.05\}$
	Talos	10^{-1}	0	N/A	$\{0.1\}$	10^{-3}	10^{-6}	N/A	$\{0.1\}$
LGCN	BPR	10^{-3}	10^{-6}	N/A		10^{-3}	10^{-6}	N/A	
	AATP	10^{-1}	0	N/A	$\{10^{-2}\}$	10^{-1}	0	N/A	$\{10^{-2}\}$
	RS@K	10^{-1}	0	N/A	$\{0.1, 5\}$	10^{-3}	10^{-6}	N/A	$\{0.15, 4\}$
	SmoothI@K	10^{-3}	10^{-8}	N/A	$\{0.15, 0.05\}$	10^{-3}	10^{-8}	N/A	$\{0.15, 0.1\}$
	SL	10^{-1}	0	N/A	$\{0.2\}$	10^{-2}	0	N/A	$\{0.2\}$
	BSL	10^{-1}	10^{-8}	N/A	$\{0.05, 0.2\}$	10^{-2}	0	N/A	$\{0.1, 0.2\}$
	PSL	10^{-1}	0	N/A	$\{0.1\}$	10^{-3}	10^{-8}	N/A	$\{0.1\}$
	AdvInfoNCE	10^{-1}	0	N/A	$\{20, 15, 10^{-5}, 0.2\}$	10^{-2}	0	N/A	$\{15, 30, 10^{-5}, 0.2\}$
	LLPAUC	10^{-2}	10^{-6}	N/A	$\{0.1, 0.1\}$	10^{-3}	10^{-6}	N/A	$\{0.5, 0.01\}$
	Talos	10^{-1}	0	N/A	$\{0.1\}$	10^{-1}	0	N/A	$\{0.1\}$
XSimGCL	BPR	10^{-3}	10^{-6}	0.1		10^{-3}	10^{-5}	0.2	
	AATP	10^{-2}	10^{-8}	0.01	$\{10^{-2}\}$	10^{-3}	10^{-8}	0.01	$\{10^{-2}\}$
	RS@K	10^{-3}	10^{-8}	0.01	$\{0.15, 5\}$	10^{-2}	10^{-6}	0.01	$\{0.1, 4\}$
	SmoothI@K	10^{-1}	0	0.01	$\{0.15, 0.05\}$	10^{-3}	10^{-8}	0.01	$\{0.1, 0.1\}$
	SL	10^{-2}	0	0.01	$\{0.2\}$	10^{-1}	0	0.01	$\{0.2\}$
	BSL	10^{-2}	0	0.01	$\{0.05, 0.2\}$	10^{-2}	0	0.01	$\{0.25, 0.25\}$
	PSL	10^{-2}	0	0.01	$\{0.1\}$	10^{-2}	0	0.01	$\{0.1\}$
	AdvInfoNCE	10^{-2}	0	0.01	$\{15, 20, 10^{-4}, 0.2\}$	10^{-3}	0	0.01	$\{15, 30, 10^{-5}, 0.2\}$
	LLPAUC	10^{-3}	10^{-6}	0.01	$\{0.6, 0.05\}$	10^{-2}	10^{-6}	0.05	$\{0.7, 0.01\}$
	Talos	10^{-2}	10^{-8}	0.01	$\{0.1\}$	10^{-1}	0	0.01	$\{0.1\}$